國立交通大學
生物科技學系
博士論文

霍氏格里蒙菌熱穩定性溶血素造成活體內外肝臟毒性的探討

Thermostable direct hemolysin from *Grimontia hollisae* causes *in vitro* and *in vivo* hepatotoxicity

研究生：林晏任

Student: Yan-Ren Lin

指導教授：吳東昆 博士

Advisor: Prof. Tung-Kung Wu Ph.D

中華民國一O二年二月

霍氏格里蒙菌熱穩定性溶血素造成活體內外肝臟毒性的探討

Thermostable direct hemolysin from *Grimontia hollisae* causes *in vitro* and *in vivo* hepatotoxicity

研究生：林晏任　**Student: Yan-Ren Lin**

指導教授：吳東昆 博士　**Advisor: Prof. Tung-Kung Wu Ph.D**

國立交通大學

生物科技學系

博士論文

A Dissertation

Submitted to Institute of Biological Science and Technology,

National Chiao Tung University,

in Partial Fulfillment of the Requirements

for the Degree of Doctor of Biological Science and Technology Hsinchu,

Taiwan, Republic of China

Feb, 2013

中華民國一〇二年二月

摘要

霍氏格里蒙菌(*G. hollisae*)已經被證實會產生熱穩定性溶血素(Gh-TDH)。以往的研究指出此毒素在人體會經由腸胃吸收，造成消化道的傷害，尤其在小腸是格外劇烈。然而，熱穩定性溶血素除了會在小腸吸收外，更有可能經由門脈循環(portal system)的靜脈回流侵犯肝臟造成二次傷害，但此關係卻從未被研究過。在本研究中，我們將進行熱穩定性溶血素造成活體內外肝臟毒性(*in vitro and in vivo* hepatotoxicity)的探討。我們使用純化的 *G. hollisae* recombinant thermostable direct hemolysin (Gh-rTDH)來進行肝毒性的分析。在活體外培養老鼠肝臟細胞株(FL83B cell line)和人類正常肝臟細胞(primary human liver cell)來測試此毒素後發現，此毒素對老鼠和人類的肝臟細胞均造成劇烈的傷害。在接觸此毒素後，肝臟細胞出現細胞質流失和皺縮等(loss of cell cytoplasm with cell shrinkage)型態上的改變，並且最終造成細胞死亡。細胞毒性測試(MTT assay)的結果顯示當毒素濃度超過 10^{-6} μg/ml 則開始顯著造成肝細胞死亡，作用時間越長或毒素的濃度越高，則毒殺肝細胞的作用就更為明顯(dose and time dependent)。Gh-rTDH 在結合異硫氰酸螢光素(fluorescein isothiocyanate-conjugated)之後被用來定位細胞受侵犯的部位，我們發現此毒素起初會圍繞肝細胞，最後將進入細胞內並且侵犯細胞核造成細胞死亡。另外，在活體內的實驗中，我們讓若干數量的小鼠(BALB/c)口服單次且不同劑量的熱穩定性溶血素或霍氏格里蒙菌，並且進行抽血分析以評估其肝臟功能。結果發現這些老鼠的肝臟酵素(glutamic-oxaloacetic transaminase /

glutamic-pyruvic transaminase)、膽紅素(bilirubin)、白蛋白(albumin)、球蛋白(globulin)在餵食毒素或細菌後均發生顯著異常，肝臟酵素在餵食後第八小時上升至最高峰。病理切片則證實無論是餵食毒素或直接餵食細菌，在肝臟的門脈周圍區域(periportal area)皆會遭受明顯的破壞，毒素或細菌的濃度越高，破壞越大。除此之外，此毒素對於心臟、腎臟並沒有造成顯著的傷害。最後，我們使用正子照影 ^{18}F-FDG PET (positron emission tomography)/CT (computer tomography) scan 來活體評估老鼠在餵食毒素或細菌前後之肝臟代謝功能及復原情形。結果發現老鼠在餵食毒素或細菌後，其代謝功能有顯著下降，並且在七天後可逐漸回復其功能。總結來說，本研究首次證實霍氏格里蒙菌之熱穩定性溶血素的確具有活體內外之肝臟毒性，肝臟的門脈周圍區域是此毒素主要的侵犯部位，肝臟代謝功能可在七天後逐漸回復。

Abstract

G. hollisae thermostable direct hemolysin (Gh-TDH) is produced by most strains of *G. hollisae.* This toxin has been reported to be absorbed in the intestines in humans. In addition to being absorbed by the intestine, TDH may also cause secondary injury to the liver via effects on the venous return of the portal system. However, a relationship between the TDH and the liver has not been reported or analyzed. In this study, we analyzed the hepatotoxicity of TDH *in vivo* and *in vitro* to provide insights into the acute injury and recovery stages of THD-induced hepatotoxicity in living animals. Liver cells (primary human non-cancer cell and FL83B mouse cells) were treated and mice (BALB/c) were fed with this toxin to investigate its hepatotoxicity. In this study, *G. hollisae* recombinant thermostable direct hemolysin (Gh-rTDH) was purified for further analysis. Morphological examination and cytotoxicity assays using liver cells were also performed. The morphological changes included cell detachment and a loss of cell cytoplasm with cell shrinkage. The MTT assay revealed that the cytoviability of liver cells decreased in proportion to the concentration of Gh-rTDH over different treatment durations (dose and time dependent.). Moreover, we noted that Gh-rTDH damaged liver cells *in vitro* when the concentration of Gh-rTDH exceeded 10^{-6} μg/ml. Fluorescein isothiocyanate-conjugated toxin was used to analyze the localization of this protein in liver cells. Cellular localization showed that the toxin was initially

located around the cellular margins and subsequently entered the nucleus. Mice were subjected to liver function measurements and liver biopsies following toxin treatment and wild-type bacterial infection. Liver function measurements and liver biopsies of the mice following treatment with toxin or infection with wild-type *Grimontia hollisae* showed elevated levels of transaminases and damage to the periportal area, respectively. PET (positron emission tomography)/CT (computed tomography) images were taken to assess liver metabolism during acute injury and recovery. The PET/CT images revealed that the reconstruction of the liver continued for at least one week after exposure to a single dose of the toxin or bacterial infection. In conclusion, the hepatotoxicity of Gh-TDH was firstly demonstrated. The damage was located in the periportal area of the liver, and the liver became functionally insufficient.

誌謝 (Acknowledgement)

從一位急診臨床醫師跨入生物科技這個有點熟悉但又相當陌生的領域當中。起初雖因反覆實驗失敗而充滿徬徨，但過程中我仍學習到許多基礎科學的知識、實驗的方法，最重要的是嚴謹的實驗態度。首先要感謝我的指導教授吳東昆老師，體諒我在職的身分，並在此基礎與臨床結合的題目上，給予解惑及最大的協助鼓勵。再來要感謝生科所的諸位學長姐、學弟妹的幫忙，尤其是裕國、文亮、聖慈、宜芳的全心的付出與大力的支持，如果沒有你們幫忙，整個過程是無法獨自完成的。感謝光田醫院核醫團隊對於動物影像實驗的幫忙與指導。最後，感謝彰化基督教醫院、交大應化諸位長官、師長的支持與照顧，與一路相伴的家人，你們都是我堅強的後盾，謝謝大家。

TABLE OF CONTENT

List of Figures

List of Table

Chapter 1 Introduction

1.1 *Vibrio* species caused diseases throughout the world

Diseases caused by different *Vibrio* species have been observed in large populations throughout the world, particularly in Asia, the United States, and Africa.(1-3) *V. cholera* and *V. parahaemolyticus* are the major etiological agents of *Vibrio*sis, which is associated with the ingestion of raw, undercooked, or contaminated seafood (1, 2) *Grimontia hollisae* (previously named *V. hollisae)* has been frequently reported to cause diseases in humans, including severe gastroenteritis, hypovolemia, and septicemia following the consumption of shellfish or oysters.(4-6) *Vibrio* species that are associated with human illness are listed in Table 1, together with Centers for Disease Control and Prevention (CDC) data on the number of reported cases and deaths in the United States. Previous studies reported that during warm summer months, virtually 100% of oysters will carry *V. vulnificus* and/or *Vibrio parahaemolyticus* (Figure 1); densities in US Gulf Coast oysters often exceed 10^4 organisms/g of oyster meat. Although *Vibrio*s do not appear to affect oysters, some species may be pathogenic to marine life.(1, 7, 8) Although *V. parahaemolyticus* has always been recognized as an important enteropathogen and cause human diseases. The incidence of *V. parahaemolyticus* infections had significantly increased since

1990s. This increase has been noted in multiple countries, including Japan and the United States, and appears to be associated with the appearance of a new clonal group with pandemic potential.(1, 9)

Vibrio species	Clinical presentation			No. of cases (no. of deaths)[a]
	Gastroenteritis	Wound or ear infection	Septicemia	
V. cholerae				
Epidemic (O1, O139)	++	(+)	—	5 (0)[b]
Nonepidemic	++	+	+	45 (0)
V. mimicus	++	+	—	10 (0)
V. parahaemolyticus	++	+	(+)	116 (1)
V. fluvialis	++	+	+	19 (0)
V. furnissii	++	—	—	1 (0)
V. hollisae	++	+	(+)	13 (0)
V. vulnificus	+	++	++	83 (31)[c]
V. alginolyticus	—	++	—	28 (0)
V. damsela	—	++	—	2 (0)
V. cincinnatiensis	—	—	(+)	0 (0)
V. carchariae	—	(+)	—	0 (0)
V. metschnikovii	(+)	—	(+)	1 (0)

Table 1 *Vibrio* species implicated as causes of human disease and number of deaths associated with infection with these species.(1)

NOTE:++, Most common clinical presentation; +, neither rare nor most common clinical presentation; (+), rare clinical presentation. [a]Data reflect *Vibrio* infections reported to the Centers for Disease Control and Prevention during 1999. Data are from the 24 states that reported cases; for many of these states, reporting of *Vibrio* infections is not routine, and consequently nos. may not reflect the true no. of cases.

Data were kindly provided by R. Tauxe, US Centers for Disease Control and Prevention, Atlanta. [b]Data include 4 cases associated with foreign travel. [c]The 31 reported deaths are from a group of 75 cases for which data on death were available.

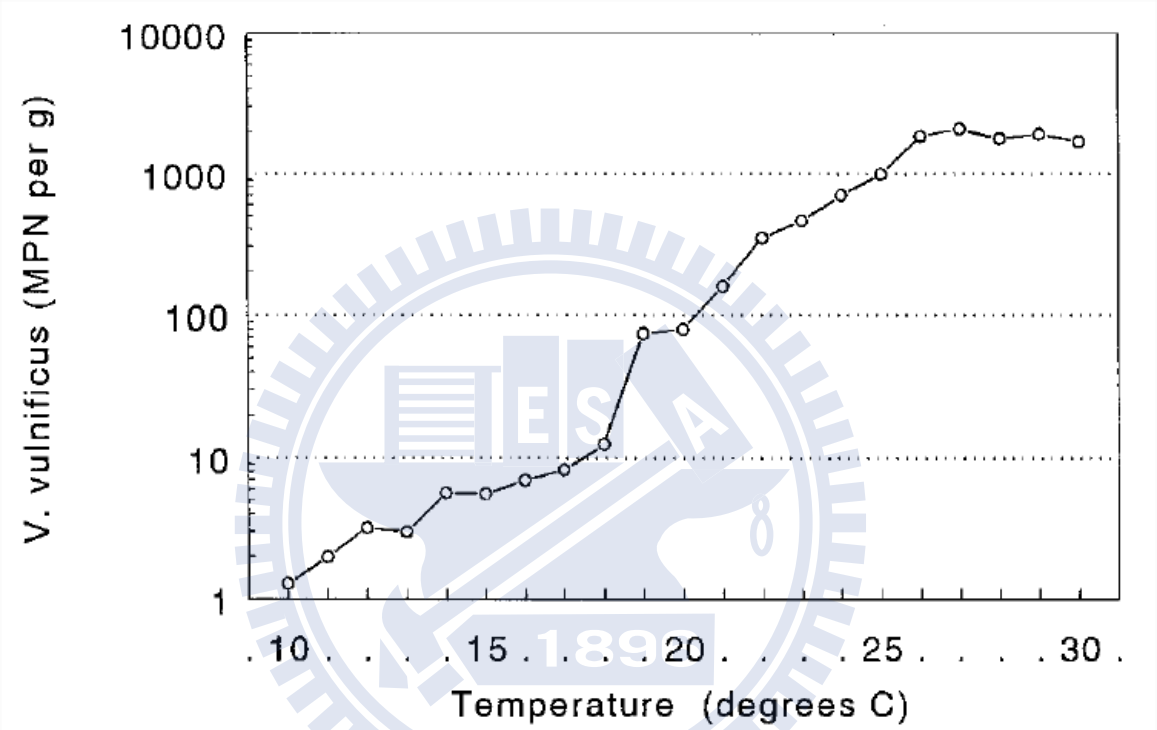

Figure 1 Influence of water temperature on the concentration of *V. vulnificus* in Gulf Coast oyster meats. Each point represents the geometric mean of all observations recorded within a 3°C temperature range.(8)

1.2 *Grimontia hollisae* cause diseases in human

G. hollisae (had ever been named *V. hollisae)* was recently and more frequently reported to cause diseases in human including severe gastroenteritis, hypovolemia and

septicemia after the consumption of shellfish and oysters.(1, 4-6, 10) *G. hollisae* was ever a species of *Vibrio* and was firstly reported by Hickman *et al.*(11) Moreover, Thompson et al. reported that *V. hollisae* strains (GenBank/EMBL accession nos AJ514909-AJ514911) shared 99.5 % 16S rDNA sequence similarity, but had only 94.6 % similarity to their closest phylogenetic neighbor, Entero*Vibrio* norvegicus. 16S rDNA sequence similarity of *V. hollisae* and *Vibrio cholerae* was only 91 %. Therefore, these results suggest that *V. hollisae* should be placed into a novel genus as *G. hollisae*.(12) This organism is reported to not usually grow on TCBS agar or Mac-Conkey agar but does grow well on sheep blood agar and marine agar.(13) However, the mechanism of morbidity caused by *G. hollisae* had not been well addressed. Although some specific laboratory examinations have been shown to be the way to detect *G. hollisae* but the incidence was still highly suspected to be underestimated because of the detecting techniques were not very popular throughout the world.(11, 13, 14)

1.3 Thermostable direct hemolysin was a violence factor

Thermostable direct hemolysin (TDH) was well known as a toxin constituted of 165 amino acid residues and which performed a variety of biological activities including hemolytic activity, cytotoxicity and enterotoxicity (Figure 2).(14, 15)

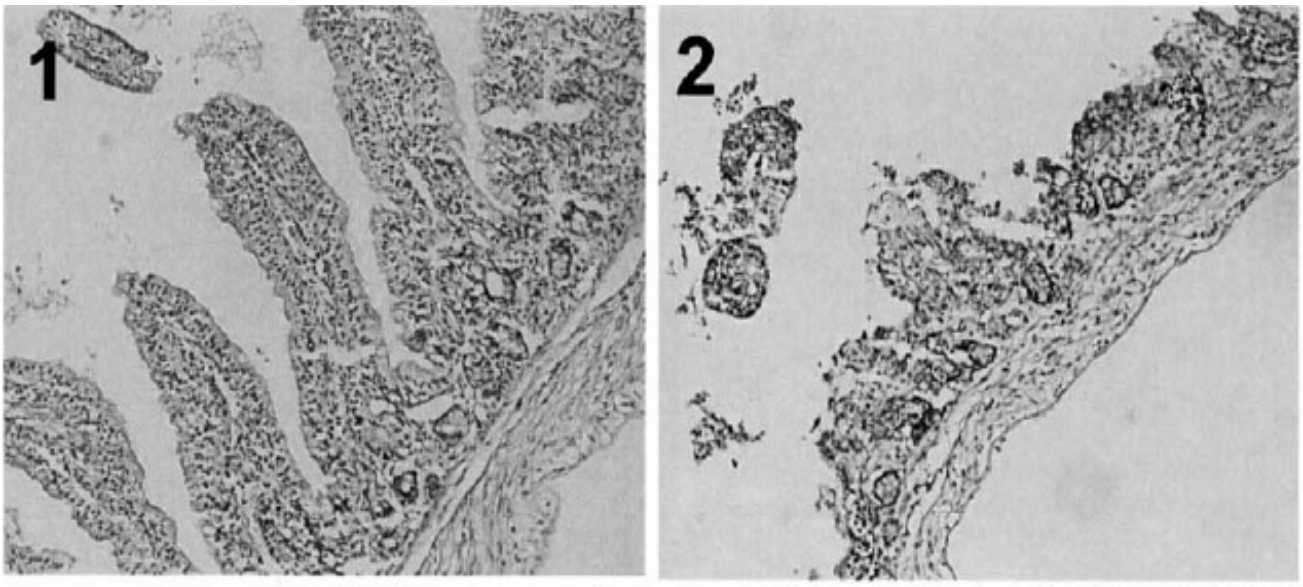

Figure 2 TDH from *V. parahaemolyticus* damaged the intestine. **(**1) PBS was treated to the intestine of rabbit and did not cause damages. (2) TDH from *V. parahaemolyticus* damaged the intestine where lumens suffered edema and hemorrhage.(15)

Some previous study reported that TDH is detoxified by aggregation into fibrils after being heated at 60-70 °C, which can be reversibly refolded into the toxic native form by being rapidly cooled after unfolding at higher temperatures (Figure 3).(16, 17)

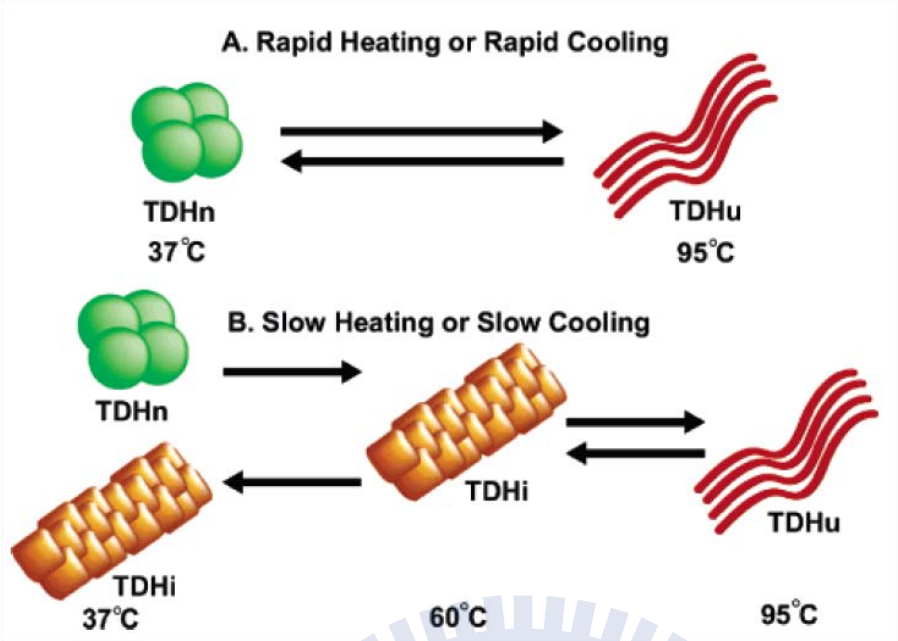

Figure 3 Model of heat-induced conformational change of TDH. Rapid heating and cooling (A) slow heating and cooling (B).(16) TDHn: native TDH; TDHu: unfolded TDH; TDHi: intermediate of TDH with fibrillar structure

The hemolytic activity of TDH is suppressed by the addition of Congo red, a dye known to be sensitive to amyloid fibrils.(16, 17) These findings support the idea that the conformational change in TDH, with the increase in β-sheet content, in a cellular membrane, may be associated with its cytotoxicity. The toxin effects of TDH had been identified from a variety of *Vibrio* species, including *V. cholera* non-O1, *V. parahaemolyticus*, *V. mimicus*, *V. alginolyticus*, and *G. hollisae*.(18-22) Among them, the production of TDHs were reported to present with similar *thd* gene sequences and pathogenesis.(21, 23) However, *tdh* gene could be noted in all strains of *G. hollisae*

but not in other *Vibrio* species.(18) In addition, the lipophilic effect of Gh-TDH is still not clearly discussed in current reports. The toxic effects of TDH have been reported to be mainly localized to the intestinal portion of gastrointestinal (15, 17, 24). However, a relationship between TDH and the liver has not been reported or analyzed. TDH might not only be absorbed by the intestine but may also cause secondary injury to the liver via effects on the venous return of the portal system. In this study, we aimed to analyze the hepatotoxicity of TDH using *in vivo* and *in vitro* analyses and to provide evidence regarding the acute injury and recovery stages of THD-induced hepatoxicity in living animals.

1.4 Research summary

Previous studies emphasized the toxin effect of TDH mainly located in the intestine of gastrointestinal tract.(15) However; the relationships between TDH and liver had not been reported or analyzed. TDH might not only be absorbed by intestine but also probably caused secondary injury to the liver via venous return of portal system (Figure 4). In this study, we aim to analyze the hepatotoxicity of TDH and *G. hollisae* (toxin and infection model) by *in vitro* (Figure 5) and *in vitro* (Figure 6) analyses and provide an evidence to report the acute injury and recover stages of liver in living animals by ^{18}F-FDG PET (positron emission tomography)/CT (computer tomography) scan.

Figure 4 TDH might not only be absorbed by intestine but also probably caused secondary injury to the liver via venous return of portal system.

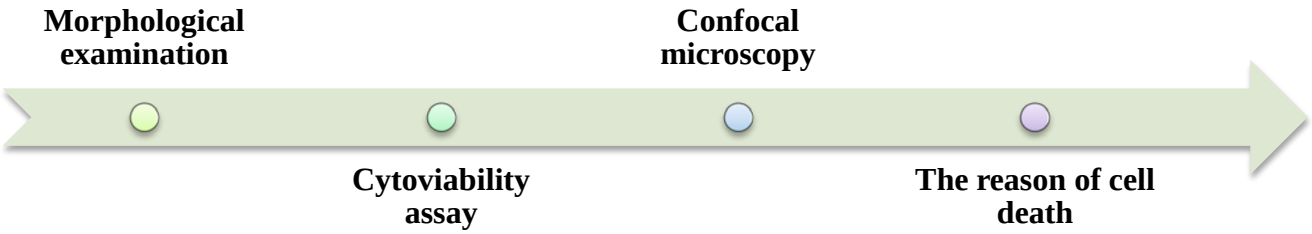

Figure 5 The parameters in analyzing the *in vitro* hepatotoxicity of TDH from *G. hollisae.* Mouse and human liver cell served as an *in vitro* model.

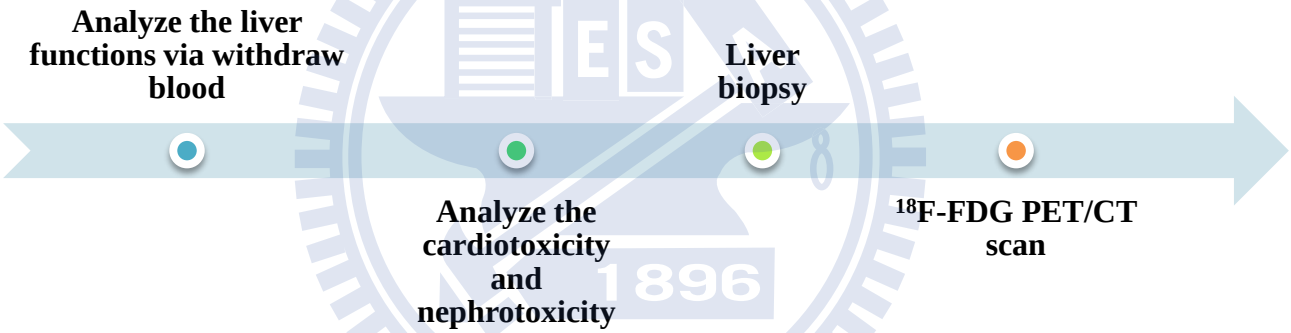

Figure 6 The parameters in analyzing the *in vivo* hepatotoxicity of TDH from *G. hollisae* and *G. hollisae.* BALB/c served as an *in vivo* model.

Chapter 2 Materials and Methods

2.1 Bacterial strains and materials

The *G. hollisae* strain ATCC 33564 was obtained in a freeze-dried form from the Culture Collection and Research Center (Hsin-Chu, Taiwan). Phenyl Sepharose 6 Fast Flow and protein molecular weight standards were purchased from GE Healthcare (Piscataway, NJ). The protein assay kits were obtained from Bio-Rad (Hercules, CA). Protein purification chemicals were obtained from Calbiochem (La Jolla, CA).

2.2 Molecular cloning, protein expression and purification, and characterization of *G. hollisae* recombinant thermostable direct hemolysin (Gh-rTDH)

The *G. hollisae tdh* gene was obtained via PCR using *G. hollisae* genomic DNA as the template and two primers, YKW-hol-TDH-N1 (5'-ATGAAATACAGACATCT-3') and YKW-hol-TDH-C1 (5'-TTATTGTTGAGATTCAC-3'). PCR reaction was carried out under the following conditions: denaturation at 94 °C for 5 min followed by 35 cycles of denaturation at 94 °C for 15 s, annealing at 58 °C for 1 min, and extension at 72 °C for 1 min followed by a final extension at 72 °C for 10 min. The amplified DNA fragment was cloned into pCR2.1-TOPO (Invitrogen, Carlsbad, CA) vector in order to construct the

recombinant plasmid pCR2.1®-TOPO-*Gh-tdh*. The recombinant plasmid was sequenced using an ABI PRISM® 3100 Genetic analyzer according to the manufacturer's protocol (Applied Biosystems, Foster City, CA).

The pCR2.1-TOPO-*Gh-tdh* plasmid harboring the *tdh* gene was transformed into *Escherichia coli* BL21(DE3)(pLysS) cells (Promega, Madison, WI) for recombinant protein production and purification. In parallel, the pCR2.1-TOPO plasmid was used as a negative control. Colonies were inoculated into Luria-Bertani broth supplemented 50 g/mL kanamycin and grown for 16 hours at 37 °C. The cells were harvested by centrifugation at 6,000 x g for 30 min, and then resuspended in 40 mL of 20 mM Tris-HCl (pH 7) buffer. The mixture was sonicated, and the cell debris was removed by centrifugation at 12,000 x g for 30 min at 4 °C. Purification method was according to a previously described method.[25] Overall, the supernatant containing produced Gh-rTDH protein was loaded on a Phenyl-Sepharose 6 Fast Flow column pre-equilibrated with 20 mM Tris-HCl (pH 7) and eluted with a linear 0 to 50% ethylene glycol gradient. Fractions exhibiting hemolysis were pooled, dialyzed, and added with NaCl to a 200 mM concentration. The active sample was applied to a Phenyl-Sepharose 6 Fast Flow column with 20 mM Tris-HCl (pH 7) and then eluted with 4 void volumes of a step gradient consisting of 200, 100, 50 mM NaCl and 20 mM Tris-HCl (pH 7) buffers. Finally, the protein (Gh-rTDH) was eluted by a 20 mM

Tris-HCl buffer and the Gh-rTDH was dialyzed against 0.1M PBS buffer (Na_2HPO_4, NaH_2PO_4, NaCl, pH 7.1) at 4°C overnight for cell and animal experiments. The molecular cloning, protein expression, and purification of Gh-rTDH were performed according to previous reports (17, 24). The effect of endotoxin has been excluded before the experiment started. In this study, the endotoxin contamination had been excluded during protein preparation by the method of anion-exchange chromatography using diethylaminoethane (DEAE) chromatographic matrices.(25, 26) Other prevention strategies including staff education (the use of aseptic technique, understanding the nature of contamination, and good housekeeping), and sterility tests were routinely performed before the study started.

2.3 Protein electrophoresis, detection and confirmed by MALDI-TOF/TOF mass spectrometry

For sodium dodecylacrylamide gel electrophoresis (SDS-PAGE), the protein sample was mixed with 5 x sample treatment buffer (125 mM Tris-HCl, pH 6.8, 2% SDS, 10% glycerol, 5%-merceptoethanol, and 0.05% bromophenol blue), and heated at 100 °C for 10 min. Electrophoresis was performed according to the manufacturer's instructions. After electrophoresis, the gel was soaked in Coomassie Blue R 250 staining solution for 30 min, then the gel was destained with the destaining solution I

(40% methanol, 7% acetic acid) and II (5% methanol, 7% acetic acid) until the stained band was distinct against a clear background. The protein identities of SDS-PAGE bands corresponding to Gh-rTDH were confirmed by MALDI-TOF/TOF mass spectrometry.

2.4 Analyzed the *in vitro* hepatotoxicity of Gh-rTDH

2.41 Cytoviability and morphological examination of Gh-rTDH treated human liver cell and FL83B cells

FL83B (BCRC 60325) and primary human non-cancer cell (kindly provided by the Liver Transplantation Center of one medical center in central Taiwan; IRB number: 120305) were cultured for use in these studies. Following attachment, the cells were treated with Gh-rTDH at a concentration of 1 μg/ml for 24 hours at 37 °C; the treating dose was determined according to the initial results of the IC_{50} determination (1 μg/ml, obtained from MTT assay). Images of the experimental group, cellular morphology were recorded microscopically at 4 time points (before Gh-rTDH exposure and after exposure to Gh-rTDH for 8, 16, and 24 hours). In addition, cells treated with PBS (mixed with culture medium) were served as control group, they were also observed at the same time points with the experimental group. All experimental or control groups under the same conditions. Hygromycin was not used in this study.

2.42 Cytoviability assay

Cytoviability of human liver cell and FL83B cells were measured by the MTT assay using 4 treatment durations (12, 16, 24 and 48 hours). In the MTT assay, cells were treated with PBS as control groups and treated with Gh-rTDH at different concentrations (10 to 10^{-8} μg/ml mixed with culture medium and administered in a total volume of 250 μl). For control group, the same concentration of vehicle was added to the culture medium. After culture for different treating durations (12hours, 16hours, 24hours and 48hours), cells were incubated with MTT for another 4 hours at 37°C. Overall, the medium was removed and DMSO was added into each well. The absorbance of the samples was measured at 570 nm using a microtiter plate reader. All experiments were performed independently for five times

2.43 Confocal microscopy

Confocal microscopy was used to investigate the locations where Gh-rTDH invaded in liver cells. Gh-rTDH was conjugated with fluorescein isothiocyanat (FITC) (emission 488nm, green) as Gh-rTDH-FITC and the reactions were performed using the FluoReporter FITC Protein Labeling Kit (molecular probes) according to the manufacturer's protocol. FL83B cells were seeded in 8-well chamber slide (1×10^4

cells/well) and incubated in the culture medium to attach. After cells were attached, they were treated with 10 μg/ml of Gh-rTDH-FITC mixed with culture medium for 20 and 40 min in darkness. Subsequently, the cells were washed 3 times using PBS (SIGMA) buffer and they were also stained with propidium iodide (PI) (SIGMA) (emission 650 nm, red) with working solution 5mg/ml in PBS for 5 min in darkness. Finally, the cells were washed 3 times using PBS buffer and observed at 26 °C by confocal microscopy (Olympus FV300).

2.44 TUNEL assay

TUNEL assay was performed for analyzing the reason of cell death. FL83B cells were respectively administrated with 1 μg/ml of Gh-rTDH for 24 hours and PBS (control group) and the result of TUNEL assay according to the manufacturer's protocol (ApoAlert® DNA Fragmentation Assay Kit) and were observed by confocal microscopy (Olympus FV300).

2.5 Analyzed the *in vivo* hepatotoxicity of Gh-rTDH

2.51 BALB/c served as an in vivo model

A total of 114 female mice aged 6 weeks were obtained from the National Laboratory Animal Center of Taiwan and were used to analyze *in vivo* hepatotoxicity.

All mice were fed normal diets. This study was carried out in strict accordance with the recommendations in the Guide for the Care and Use of Laboratory Animals of the National Institutes of Health. The protocol was approved by the Committee on the Ethics of Animal Experiments of the National Chiao Tung University (Permit Number: 01001008). All surgery was performed under sodium pentobarbital anesthesia, and all efforts were made to minimize suffering.

2.52 Withdraw blood for analyzing the liver functions (n=25)

Twenty-five mice were divided into 5 groups (n = 5 for each group). One group served as a control group and was administered PBS; the other 4 groups were administered different dosages of Gh-rTDH (0.1, 1, 10, and 100 μg) as a single treatment. The dosage that might initiate organ injury in animals has never been reported (information on natural infection in humans is also lacking). Therefore, the treatment dosages were carefully determined and modified according to the initial results of the IC_{50} determination (1 μg/ml, obtained from the MTT assay described above). All mice were treated using the same volume (200 μl), the same treatment time (10:00 am) and via gastric tubes without volume loss (i.e., vomiting). One hundred microliters of whole blood was withdrawn from the orbital vascular plexus of each mouse using a capillary tube and no analgesics. There were 8 experimental

sampling times: before treatment with PBS or Gh-rTDH and 4, 8, 16, 32, 64, 128 and 256 hours after treatment with PBS or Gh-rTDH. The blood samples were analyzed for the continuation of liver function as assessed by glutamic-oxaloacetic transaminase (GOT), glutamic-pyruvic transaminase (GPT), total/direct/indirect bilirubin, albumin and globulin)(Reagents Beckman Coulter®). One-way ANOVA analysis was used to analyze the significant differences between each treatments/time point. All analyses were performed with the SPSS statistical package for Windows (Version 15.0, SPSS Inc., Chicago, IL).

2.53 Withdraw blood for analyzing the cardiotoxicity and nephrotoxicity (n=20)

Twenty mice were divided into 4 groups (each n=5). One of the 4 groups was served as control group which were fed with PBS and the other 3 groups were respectively fed with Gh-rTDH in dosages of 1 μg, 10 μg and 100 μg in single administration via gastric tubes (each mouse was fed at AM10:00 with total volumes of 200 μl). Each mouse was also respectively withdrawn 100 μl of whole blood at the 5 different time points: (1) before feeding with PBS or Gh-rTDH; (2) after feeding with PBS or Gh-rTDH for 4, 16, 64, and 256 hours. Their blood samples were analyzed for nephrotoxicity by detecting the level of creatinine (Assay kit: Creatinine Reagent, Beckman Coulter®; Supply: Beckman Coulter Synchron CX7 Analyzer) and

for cardiotoxicity by detecting the levels of CK-MB (Assay kit: CK-MB Reagent Pack, Beckman Coulter®; Supply: Beckman Coulter Synchron CX7 Analyzer) and Troponin I (Assay kit: ADVIA Centaur TnI-Ultra Readypack®; Supply: Bayer ADVIA Centaur). Above all, blood samples were diluted appropriately for enough volume to be detected by analyzers and were operated according to the manufacturer's protocol. One-way ANOVA analysis was also used to analyze the significant differences between each treatments/time point.

2.54 Liver biopsy (n=9)

Nine mice were divided into 3 groups, which were treated with PBS, 10 μg of Gh-rTDH or 100 μg of Gh-rTDH (n = 3 in each group) in a single administration via a gastric tube. All mice had their livers biopsied after 8 hours of treatment. Samples were prepared with H&E staining from tissue harvested at the time of animal sacrifice.

2.55 PET/CT scan (n=60)

In this study, the ^{18}F-FDG (2-fluoro-2-deoxy-D-glucose) PET /CT scan was used to take images in detection the liver cells metabolism in living animals after exposure of Gh-rTDH and their trends were recorded (GE Medical System, Discovery

ST). ^{18}F-FDG PET/CT imaging provides precise fusion of molecular PET images with high-quality anatomical CT images. Technical parameters used for CT portion of PET/CT are designed as follow: CT scan type with helical full of 0.5 second, a detector row configuration of 16x1.25mm, an interval space of 2.5 mm, the slice thickness of 1.2 mm, pitchof 1.75:1 (high quality mode), a speed of 17.5mm per rotation, scan FOV of large, voltage of 120 kVp and current of 200 mA. Technical parameters used for PET portion of ^{18}F-FDG PET/CT are designed as follow 10 min in each bed, the FOV chosen for imaging reconstruction is 20 cm and PET resolution is 4.5 mm FWHM. The reconstructive parameters are type 3D iteration.

Sixty mice were divided into 4 major groups and each group (n=15) was respectively fed with PBS, 1 μg, 10 μg and 100 μg of Gh-rTDH in single administration via gastric tubes. Among each group, mice were further grouped to receive ^{18}F-FDG PET/CT scan in different time points including the 8th (n=5), 72th (n=5) and 168th (n=5) hours after feeding with Gh-rTDH. In the study, 0.07mCi ^{18}F-FDG for each mouse was given by tail vein injection before taking the image (Figure 7A). After injection the ^{18}F-FDG, images taking were performed one hour later with appropriate general anesthesia (Isoflurane) (Figure 7B-D). In our study, each mouse did not be proposed to receive ^{18}F-FDG PET/CT scan in every time points to follow up because of recurrent general anesthesia in short time might cause severe hepatotoxicity and could

influence the results of this study. In the ^{18}F-FDG PET/CT images, the ^{18}F-FDG uptake value was calculated using region of interest (ROI). In each mouse, the ROIs of liver and muscle were recorded for semi-quantification which was proposed to be the ratios of liver/muscle ^{18}F-FDG uptake level.

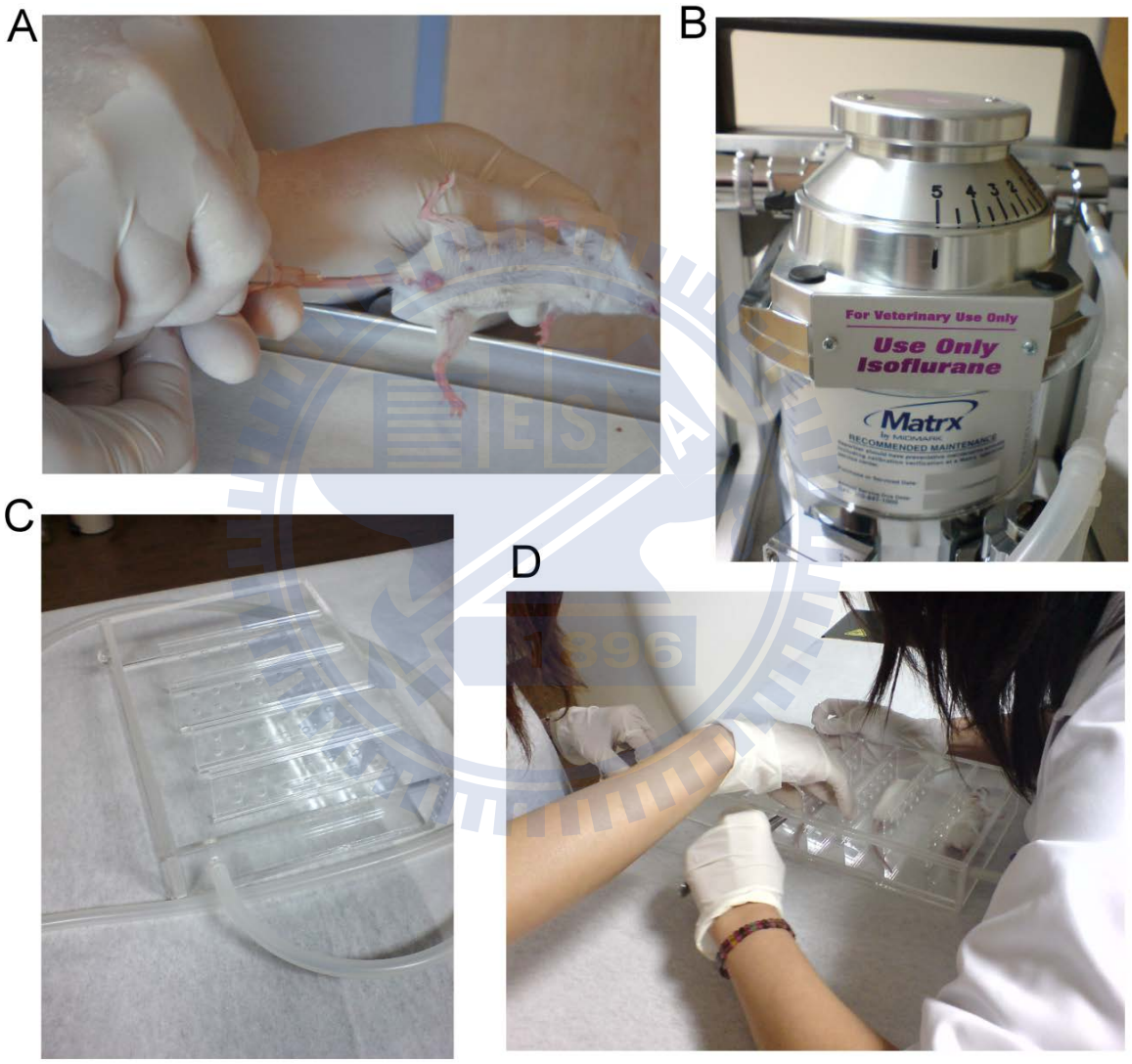

Figure 7 ^{18}F-FDG and Isoflurane were treated to each mouse before scan started. (A) ^{18}F-FDG for each mouse was given by tail vein injection before taking the images. (B)

Isoflurane was used to perform general anesthesia. (C) Mice were respectively lay down on the box and (D) received ^{18}F-FDG PET/CT scan.

2.6 Infection models –*In vivo* hepatotoxicity of the *G. hollisae* strain, Escherichia coli containing the recombinant Gh-tdh gene (*E. coli*-TOPO-tdh), and the *E. coli*-TOPO strain in BALB/c mice (n=126).

An animal infection model was set up to demonstrate the hepatotoxicity of bacterial infection. The *G. hollisae strain (wild type), E. coli*-TOPO-*tdh, and E. coli*-TOPO *strains* were cultured. Seventy-five mice were divided into three major groups (n=25 for each group) and infected with bacteria via oral administration. Two groups were infected with *G. hollisae* and *E. coli*-TOPO-*tdh* to demonstrate their hepatotoxicity; the third group was infected with *E. coli*-TOPO to serve as a control group. For each major group, five subgroups were established (n=5 for each group) according to their treatment dosage (10^7, 10^8, 10^9, 10^{10} and 10^{11} organisms/ml and treated with the same volumes. One hundred microliters of whole blood was withdrawn at 8 different time points: before treatment with bacteria and 4, 8, 16, 32, 64, 128 and 256 hours after treatment with bacteria. Blood samples were analyzed for continued liver function (GOT, GPT, total bilirubin, albumin and globulin). In addition, 6 mice were treated with 10^{11} organisms/ml of *G. hollisae*, *E. coli*-TOPO-*tdh*,

and *E. coli*-TOPO (n=2 for each group). For these animals, liver biopsies and H&E staining (200X) were performed 8 hours after bacterial treatment. Finally, 54 mice were treated with *G. hollisae*, *E. coli*-TOPO-*tdh* and *E. coli*-TOPO (n=18 for each group) with a single administration. Among each group, mice were sub-grouped for treatment with bacteria at the concentrations of 10^7, 10^9 and 10^{11} organisms/ml (n=6 for each group). In each concentration group, mice received a PET/CT scan at 8, 72 and 168 hours (n=2 for each group) after bacterial treatment.

2.7 Analyzed the *in vivo* and *in vitro* hepatotoxicity of fiber from Gh-rTDH (n=34)

In this study, fiber form of Gh-rTDH was prepared by heat treatment at 60 °C, and the aggregates were collected by centrifugation. The method of preparing fiber form of Gh-rTDH was according to a previously described method.(16) The productions of fiber form of Gh-rTDH were confirmed by testing their hemolytic ability. FL83B cells were treating with fiber form of Gh-rTDH and morphological examination and cytoviability assay were performed (procedures and conditions were uniform with previous description in the method section of 2.4). Moreover, mice (n=25) were also fed with fiber form of Gh-rTDH and their liver functions including the levels of GOT, GPT, total bilirubin, albumin and globulin were recorded. Liver

biopsy and pathological images were taken in mice (n=8) for further analyzing the hepatotoxicity of mice (procedures and conditions were uniform with previous description in the method section of 2.5).

Chapter 3 Results

3.1 Identification of the Gh-rTDH purified from *G. hollisae*

Electrophoresis of the homogeneous protein revealed a molecular mass of ~ 22 kDa as determined by the SDS-PAGE (Figure 8). Moreover, we found that tandem mass spectrum of the doubly charged tryptic peptide at *m/z* 1024.543 from SDS-PAGE of Gh-rTDH and a unique hit matching the ^{35}VSDFWTNR^{42} of Gh-rTDH peptide sequence was identified from the mass differences in the y-fragment ion series of MALDI TOF/TOF spectrum **(**Figure 9).

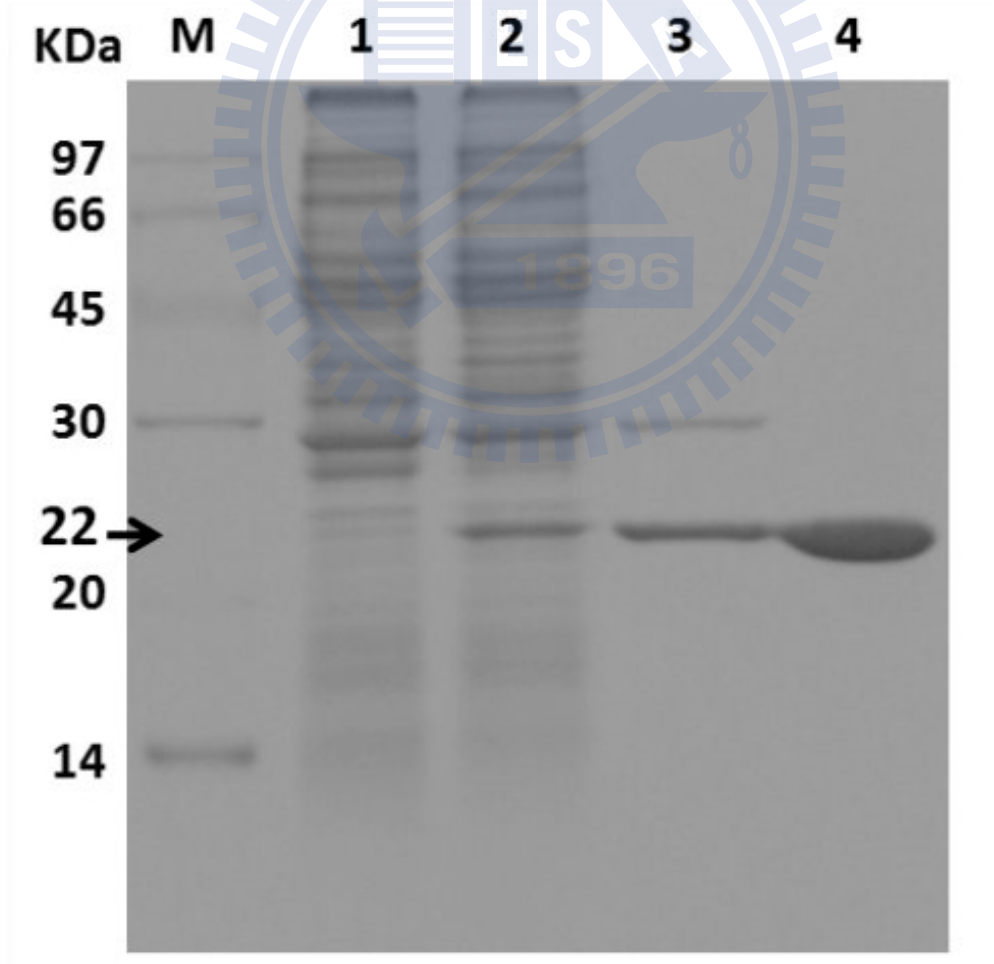

Figure 8 Purification and characterization of the Gh-rTDH protein. (A) Coomassie blue-stained SDS-PAGE of Gh-rTDH protein. Marker proteins (M): phosphorylase b (97 kDa), albumin (66 kDa), ovalbumin (45 kDa), carbonic anhydrase (30 kDa), trypsin inhibitor (20 kDa), α-lactoalbumin (14 kDa); lane 1: cell crude extract of BL21(DE3) pLysS strain containing pCR2.1-TOPO plasmid alone; lane 2: crude protein expressed from BL21(DE3) pLysS strain containing pCR2.1-TOPO-*Gh-tdh* gene; lane 3 and 4: Phenyl Sepharose 6 Fast Flow purified protein showed a homogenous protein with a molecular mass of ~ 22 kDa.

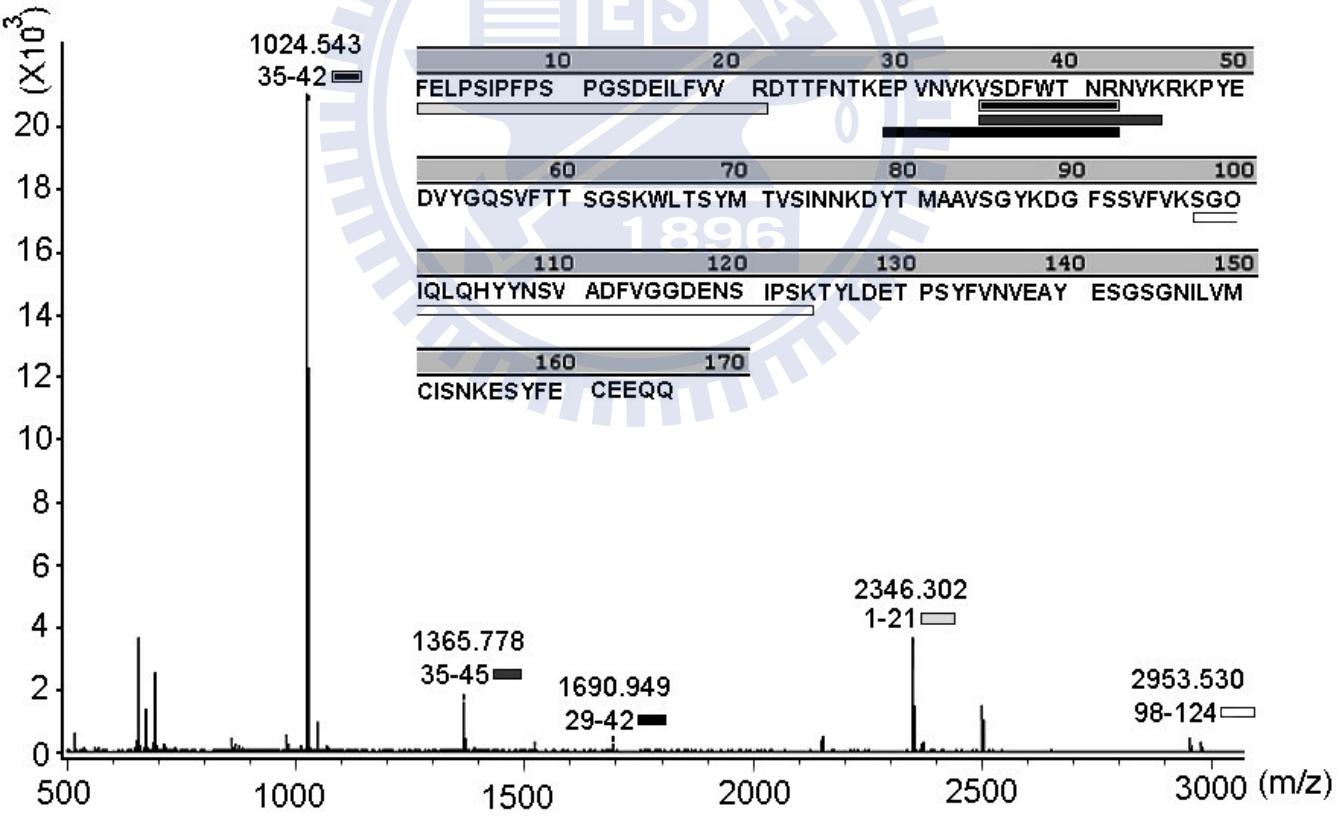

Figure 9 Tandem mass spectrum of the doubly charged tryptic peptide at *m/z* 1024.543 from SDS-PAGE of Gh-rTDH. A unique hit matching the ^{35}VSDFWTNR^{42} of Gh-rTDH peptide sequence was identified from the mass differences in the y-fragment ion series of MALDI TOF/TOF spectrum.

3.2 Gh-rTDH caused *in vitro* liver cell damage

The morphology of liver cells was obviously changed after administrating with 1 μg/ml Gh-rTDH for 24 hours at 37 °C. The morphological changes included cell detachment, and loss of cell cytoplasm with cell shrinkage (Figure 10A-D). The MTT assay also revealed that the cytoviability of liver cells decreased in proportion to the concentrations of Gh-rTDH in different treating durations. Moreover, we noted that the Gh-rTDH damaged the liver cells *in vitro* when the concentration of Gh-rTDH crossed 10^{-6} μg/ml (Figure 11). Moreover, in this study, primary human hepatocytes (non-cancer liver cells) were used to demonstrate the toxicity of Gh-TDH via MTT assay. These primary human hepatocytes were kindly provided by the liver transplantation center of a medical center in central Taiwan under IRB permission (IRB number: 120305). In this MTT assay, the Gh-TDH still caused obvious hepatotoxicity in primary human hepatocytes (Figure 12).

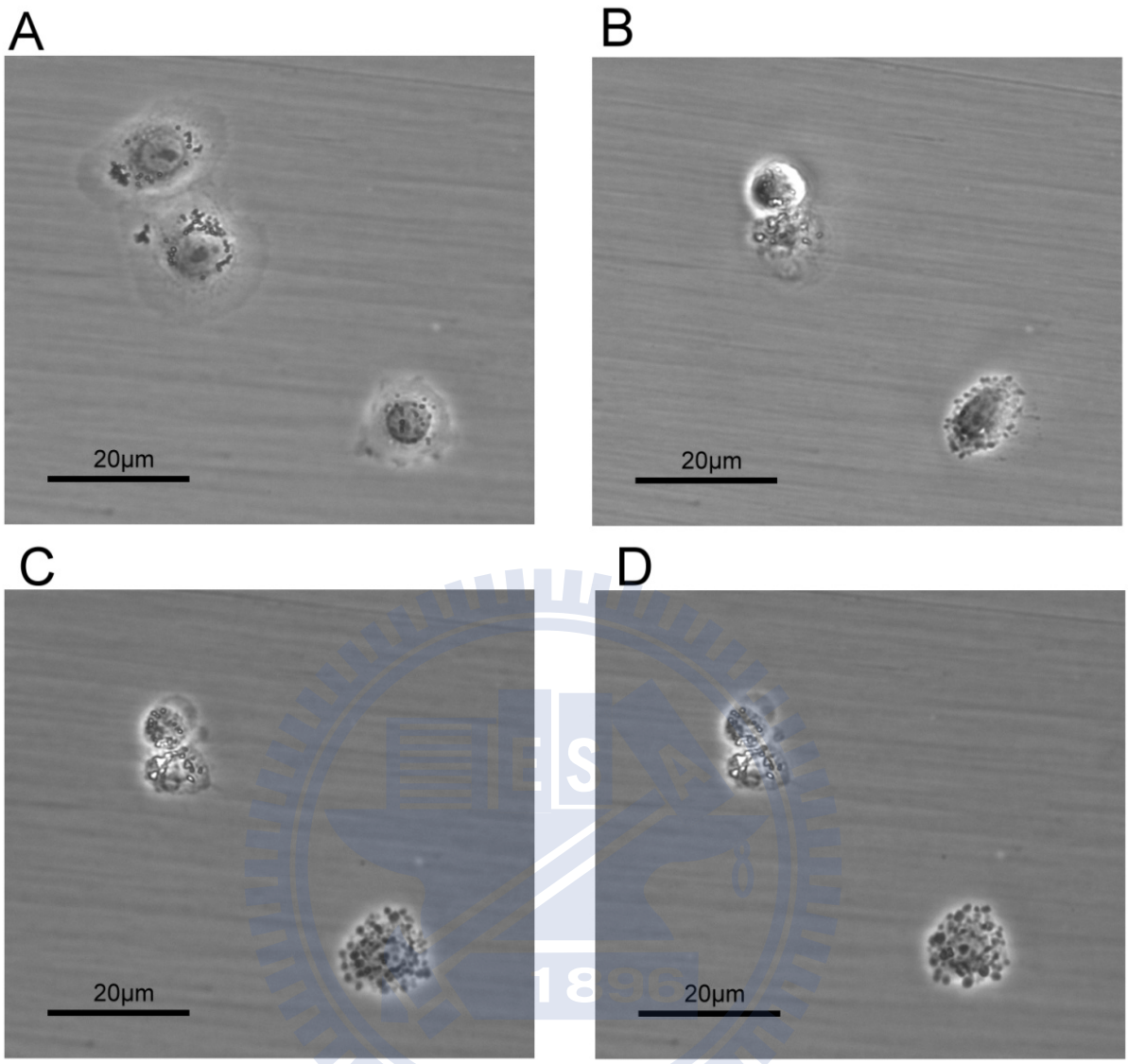

Figure 10 The morphology of liver cells (FL83B) was clearly changed after the administration of 1 μg/ml Gh-rTDH for 24 hours at 37 °C. The morphological changes included cell detachment and a loss of cell cytoplasm with cell shrinkage; they were the same cells recorded in different time points. (A) The liver cells before exposure and (B) after exposure to the Gh-rTDH protein for 8 hours, (C) for 16 hours and (D) for 24 hours.

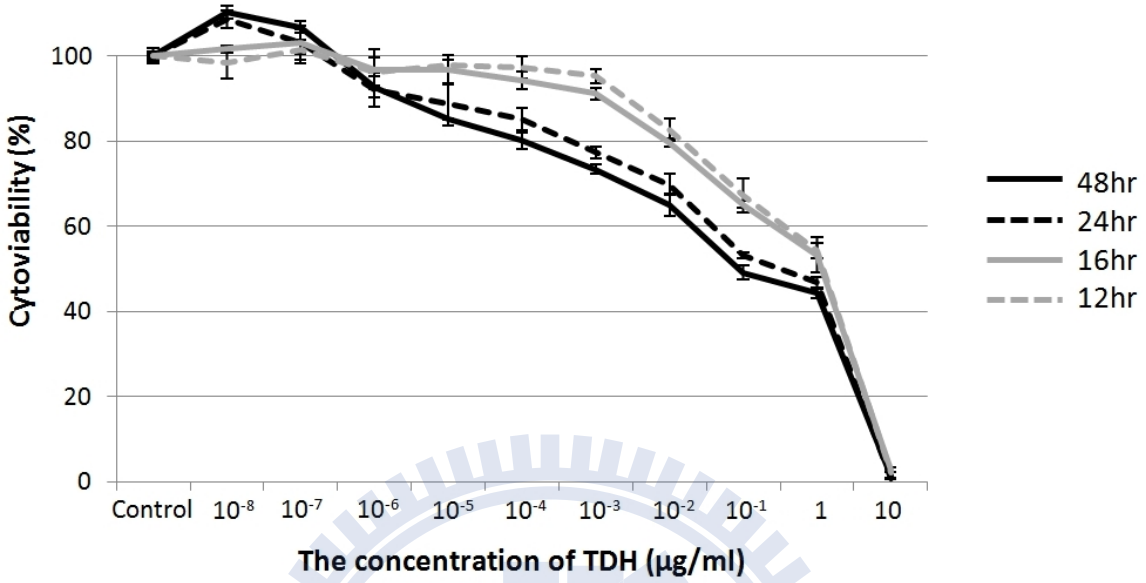

Figure 11 The MTT assay of mouse liver cells. The MTT assay revealed that the cytoviability of mouse liver cells decreased in proportion to the concentration of Gh-rTDH over different treatment durations. Moreover, we noted that Gh-rTDH damaged liver cells *in vitro* when the concentration of Gh-rTDH exceeded 10^{-6} μg/ml.

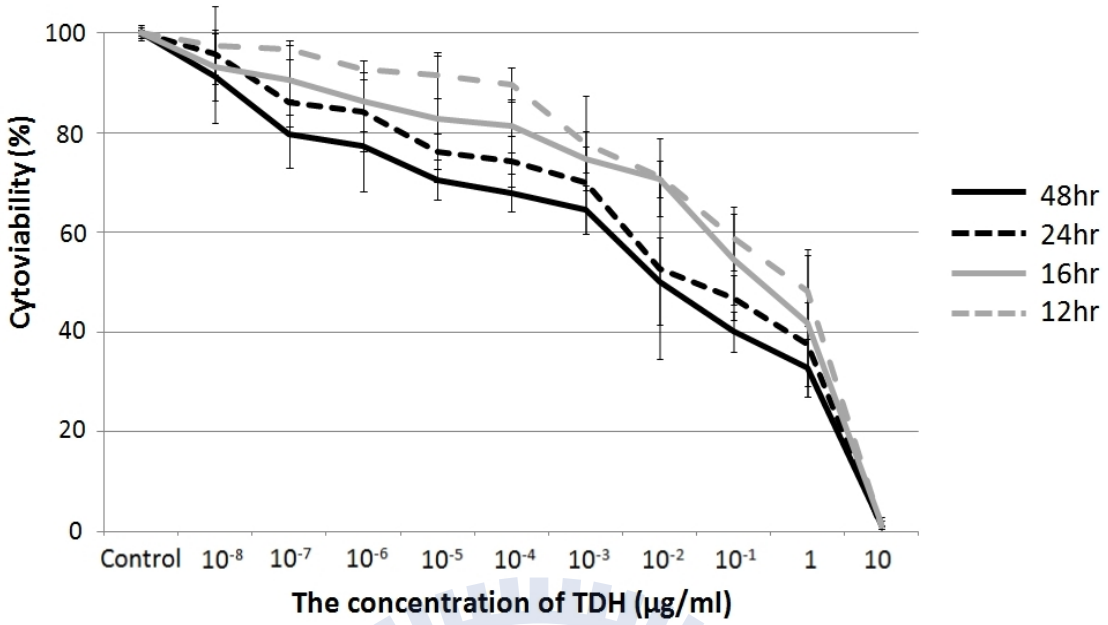

Figure 12 The MTT assay of human liver cells. The MTT assay revealed that the cytoviability of primary human hepatocytes (non-cancer liver cells) decreased in proportion to the concentration of Gh-rTDH over different treatment durations. Moreover, we noted that Gh-rTDH damaged liver cells *in vitro* when the concentration of Gh-rTDH exceeded 10^{-8} μg/ml.

3.21 Gh-rTDH-FITC bound the margin of liver cells and invaded their nucleuses

Gh-rTDH-FITC was used to demonstrate the locations where the protein invaded. The confocal microscopy with FITC filter revealed that Gh-rTDH-FITC bound around the margin of liver cells after administrating with 10 μg/ml Gh-rTDH-FITC for 20 min at 26 °C (Figure 13 A-C). Moreover, Gh-rTDH-FITC further located in the nucleus of liver cell after treating with Gh-rTDH-FITC for 40

min at 26 °C and PI was also stained for confirming the location of nucleus (Figure 13 D-F).

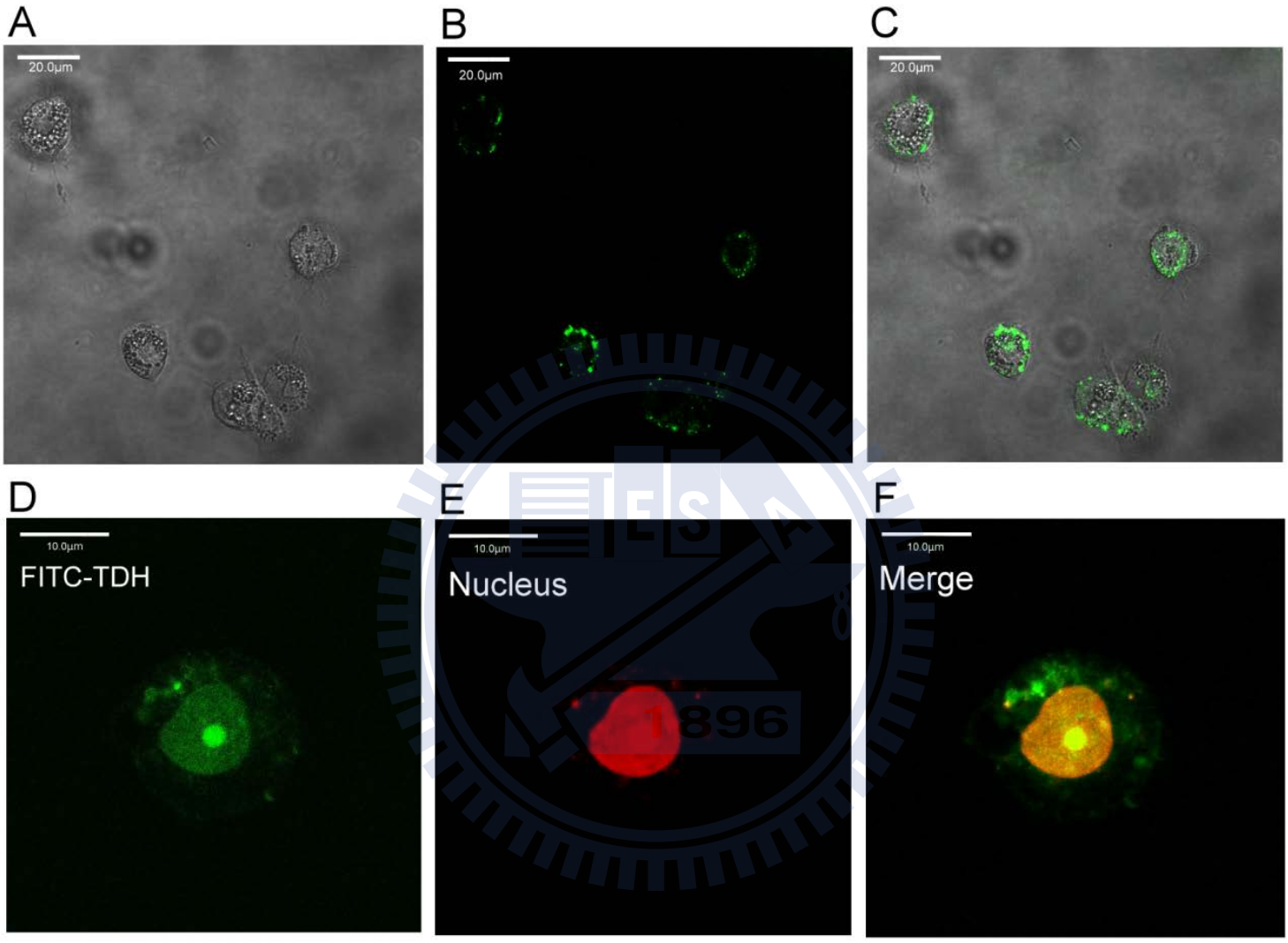

Figure 13 Subcellular localization of Gh-rTDH. The liver cells respectively administrated with 10 μg/ml Gh-rTDH-FITC for 20 (A-C) and for 40 (D-F) min at 26 °C and were observed by confocal microscopy. (A) The liver cells were observed without FICT filter (B) with FITC filter (C) merge A and C confirmed that Gh-rTDH-FITC (green) bound around the margin of liver cells. (D) The nucleus of

liver cell was invaded by Gh-rTDH-FITC (green) (E) nucleus stained with PI (red) (F) merge of D and E confirmed that Gh-rTDH-FITC was located in the nucleus of liver cell.

3.22 Gh-rTDH caused liver cells death by cell apoptosis

After treating liver cells with 1 μg/ml of Gh-rTDH for 24 hours, TUNEL assay was performed and positive findings were noted. DNA fragmentations could be noted in the cytoplasm of cells (Figure 14 A-D). In the control group, TUNEL assay was negative finding (Figure 15).

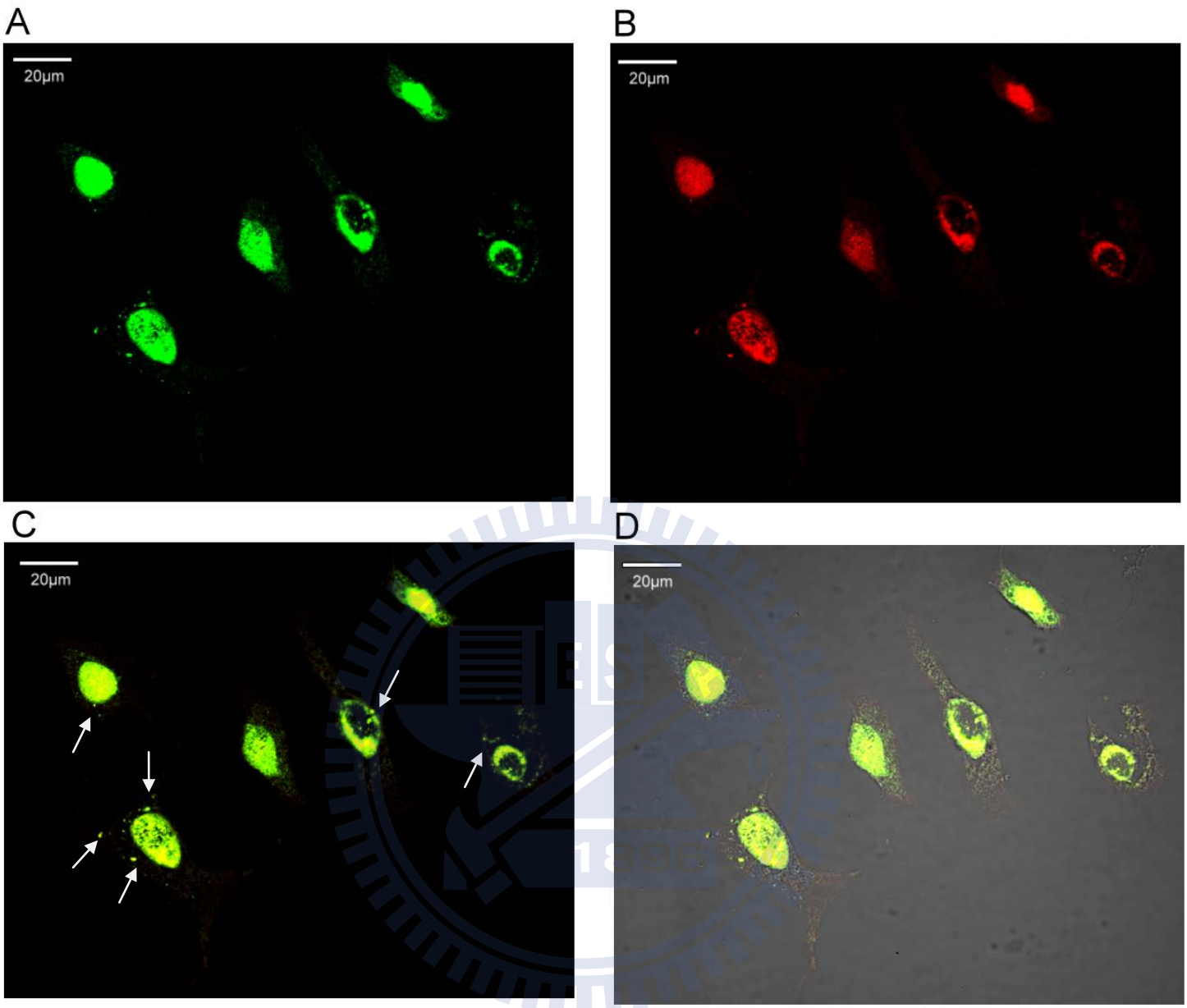

Figure 14 The liver cells were administrated with 1 μg/ml of Gh-rTDH for 24 hours and performed with TUNEL assay were observed by confocal microscopy. (A) TUNEL positive, (B) stained with PI, (C) merge of A and B, (D) merge of C and image without filter. **Arrows: DNA fragmentations**

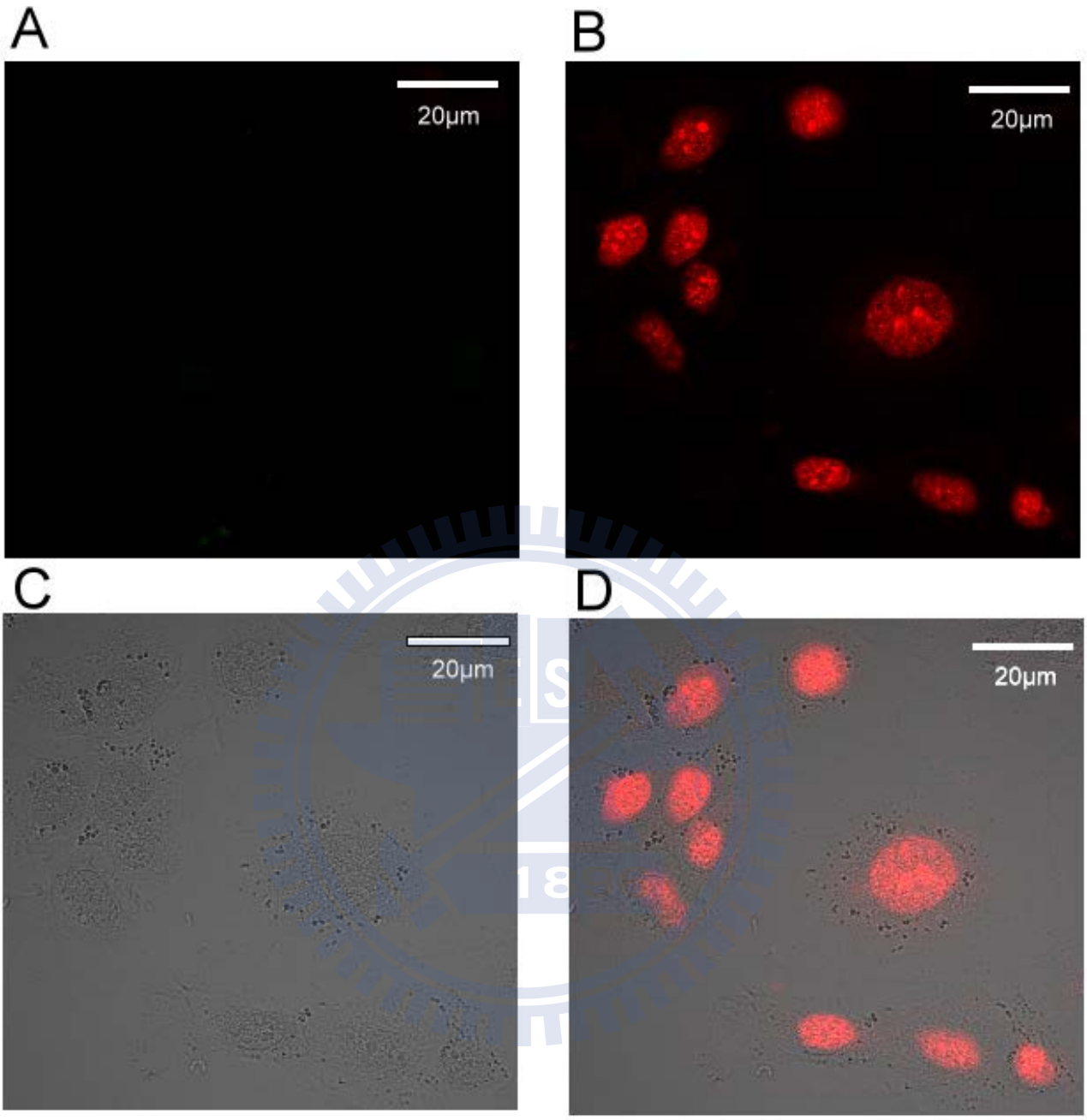

Figure 15 In the control group, the liver cells were administrated with PBS for 24 hours and performed with TUNEL assay was observed by confocal microscopy. (A) TUNEL negative, (B) stained with PI, (C) without filter, (D) merge of C and D

3.3 Liver damages *in vivo* were induced by Gh-rTDH

The levels of GOT and GPT were not elevated in the control group after the administration of a single dose of PBS. However, the mean GOT and GPT levels were clearly elevated in the group that was treated with 0.1 μg Gh-rTDH, and the highest levels were observed 8 hr after toxin administration. Similar findings were observed in other treatment groups. Higher doses of Gh-rTDH were clearly associated with more severe mouse liver injury (Figures 16).

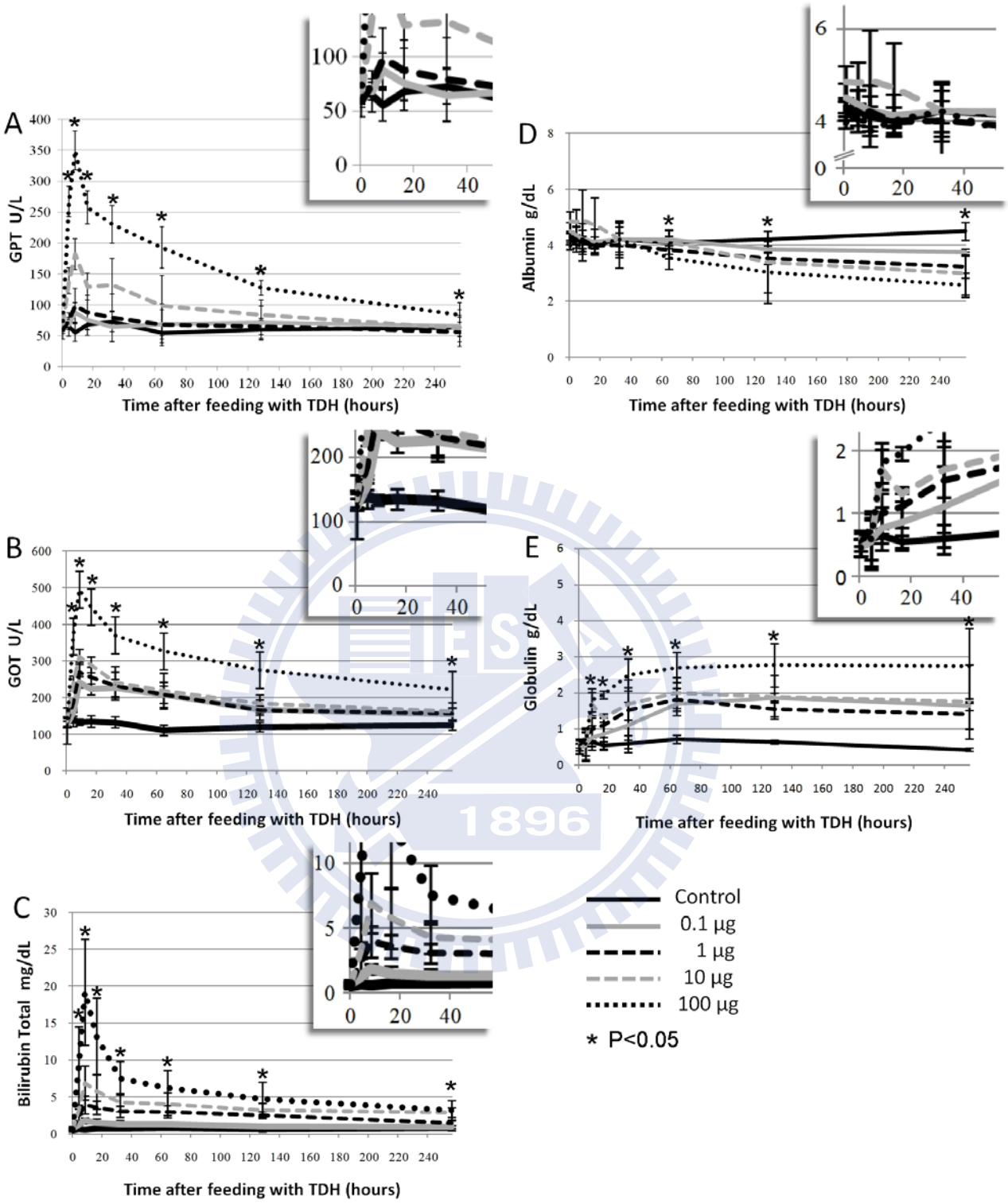

Figure 16 Liver function evaluation after a single administration of Gh-rTDH. The levels of liver function were abnormal after a single administration of Gh-rTDH. Six-week-old female BALB\c were treated with four different dosages of Gh-rTDH

(0.1, 1, 10, and 100 μg), and the control group was treated with PBS (n = 5 for each group). Acute liver injury was demonstrated by elevating the levels of (A) GPT and (B) GOT; the highest levels could be found at the 8th hr after feeding in both. (C) Hyperbilirubinemia and (D) hypoalbuminemia also occurred in the mice that were treated with Gh-rTDH. The hyperbilirubinemia was the most severe at the 8th hr, and hypoalbuminemia was noted after 32 hr of treatment with Gh-rTDH. (E) Globulin levels were gradually increased after exposure to Gh-rTDH. *A p-value < 0.05 was considered statistically significant.

3.31 Acute hemolytic status in vivo was caused by Gh-rTDH

In addition, the total bilirubin level did not change in the control group (Figure 16 C) the distributions of bilirubin were similar in different time points after exposure with PBS (Figure 17 A). However, in the groups fed with Gh-rTDH, their total bilirubin levels were obviously elevated and the higher dosage of Gh-rTDH made the levels of total bilirubin higher (Figure 17 C). Moreover, the proportions of indirect from bilirubin were much higher than the direct from of bilirubin within 8 hours after exposure with Gh-rTDH in the dosages of 1 μg and 100 μg (Figure 17 B and C). According to our findings, the acute hemolytic status *in vivo* could be induced by feeding with Gh-rTDH.

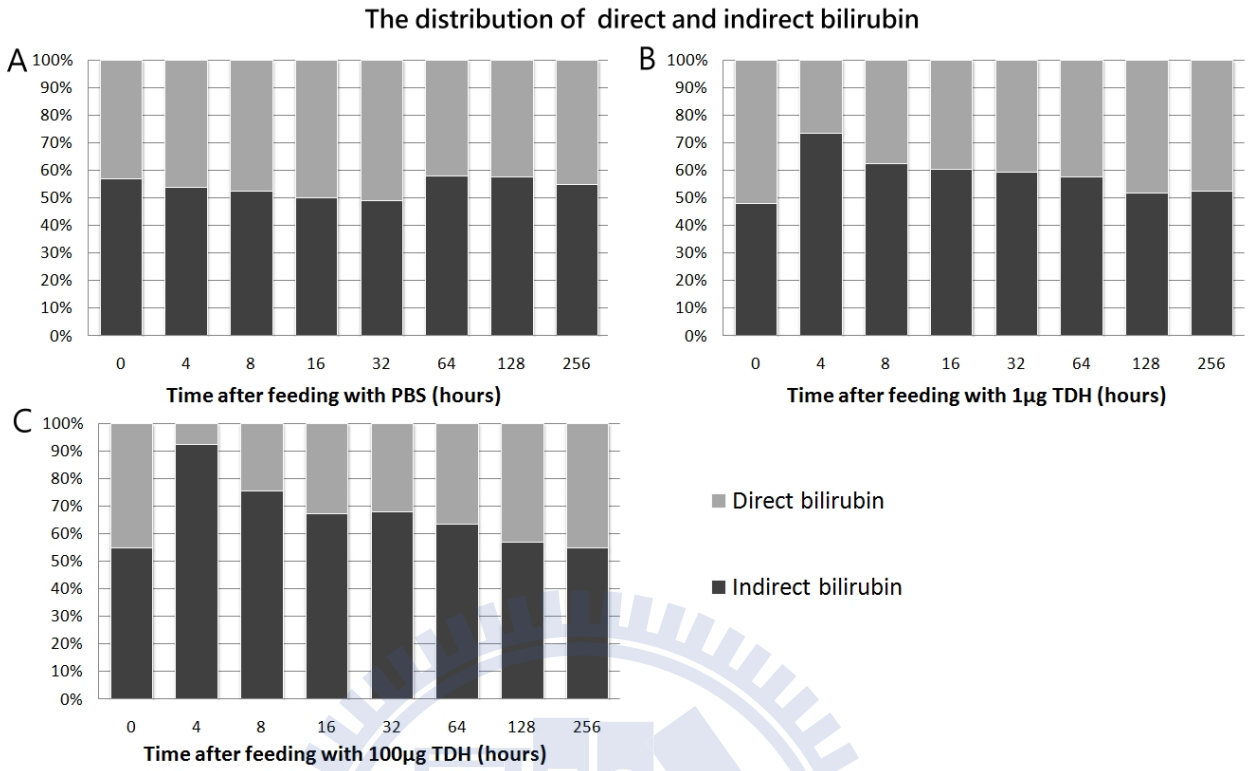

Figure 17 Gh-rTDH induces an acute hemolytic status. The distribution of direct and indirect bilirubin in mice that were fed with (A) PBS (control), (B) 1 μg of Gh-rTDH, or (C) 100 μg of Gh-rTDH. The percentages of indirect form of bilirubin were similar in different time points after exposure to PBS. In mice fed with 1 μg and 100 μg of Gh-rTDH, the percentages of indirect form of bilirubin both obviously increased in the 4th hour and gradually subsided. This result indicated that the Gh-rTDH caused acute hemolytic status *in vivo* and the severity associated with the feeding dosages of toxin.

3.32 Gh-rTDH damaged the functions of albumin synthesis in liver and triggered immune system

The albumin levels began to decrease after feeding with Gh-rTDH for 32 hours and were in proportion to the feeding dosages. Moreover, in the groups fed with Gh-rTDH, their albumin levels progressively decreased and which did not recover even in the 256th hour (Figure 16 D). These results indicated that in the mice fed with Gh-rTDH, their functions of albumin synthesis were damaged and were difficult to recover in the initial 256 hours after exposure to Gh-rTDH. In addition, the globulin levels were higher in groups fed with Gh-rTDH than in control group. This finding indicated that Gh-rTDH might trigger immune system in circulation (Figure 16 E).

3.33 Gh-rTDH might not cause in vitro cardiotoxicity and nephrotoxicity.

The creatinine and CK-MB levels which significantly and clinically reflected the kidney and heart injury were both not elevated in the groups fed with Gh-rTDH. The levels of creatinine and CK-MB did not change in proportion to the feeding dosages of Gh-rTDH. Moreover, the Troponin I levels were also normal in all mice fed with Gh-rTDH (Figure 18).

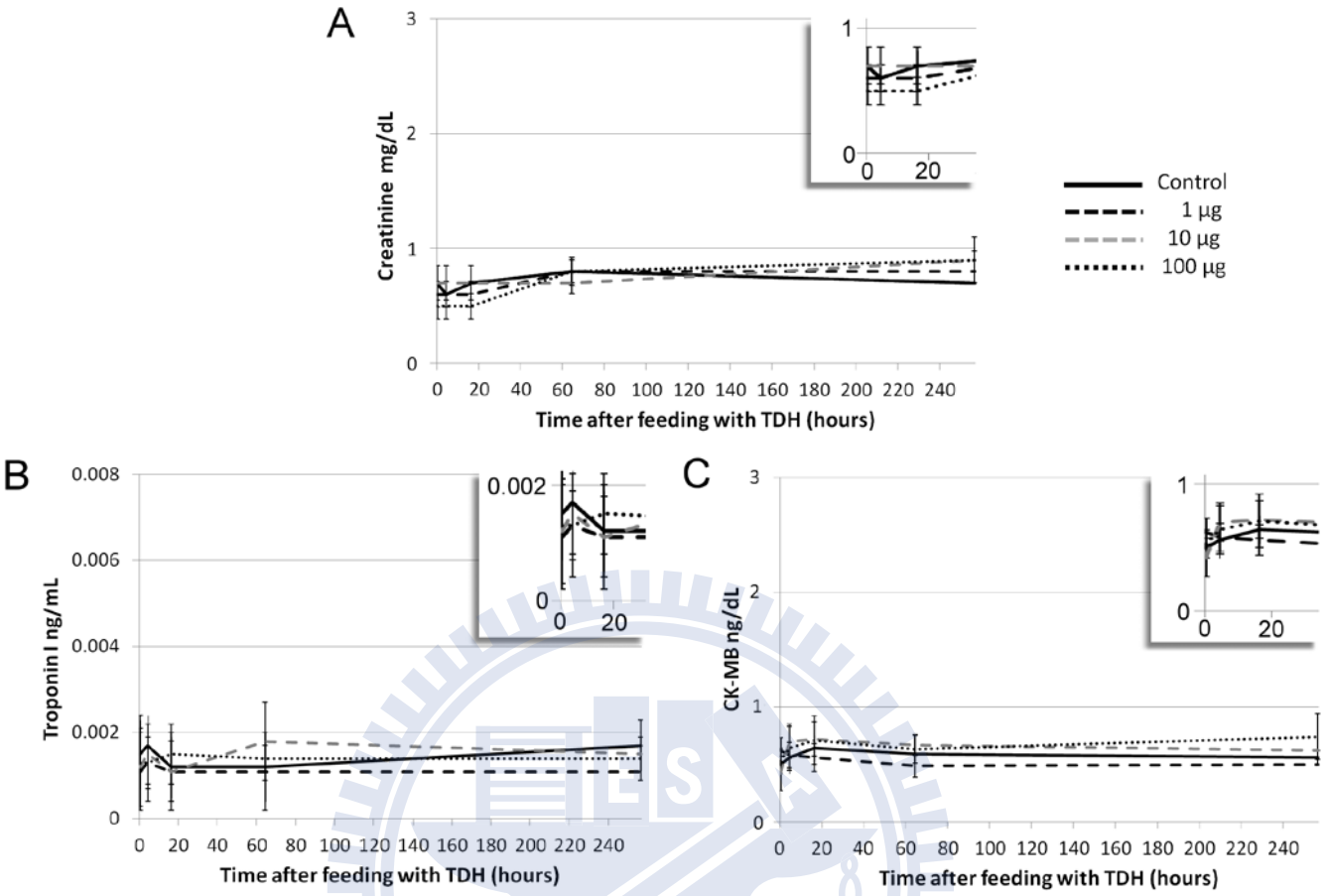

Figure 18 Gh-rTDH might not cause cardiotoxicity and nephrotoxicity. Cardiotoxicity and nephrotoxicity were surveyed by withdrawing blood. Mice were respectively fed with three different dosages of Gh-rTDH (1 μg, 10 μg and 100 μg) and control group was fed with PBS (each group n=5). Their levels of (A) creatinine and (B) CK-MB were both normal in the serum of mice after single exposure to Gh-rTDH.

3.34 Liver biopsy demonstrate that the damages located in the periportal area of liver

In the control group, the liver biopsy was performed and normal liver parenchyma without pathological change was noted (Figure 19 A and B). However, in mice fed with 10 μg of Gh-rTDH, the liver biopsy demonstrated the preserved liver parenchyma architecture with mild congestion over the periportal areas at the low power magnification, and spotty liver cells damage around the portal vein at the high power magnification. These damages were obviously located in the periportal area (zone 1 of the liver acinus) (Figure 19 C and D). Moreover, in mice fed with 100 μg of Gh-rTDH, severe congestion with hemorrhage were noted at the low power magnification and high power magnification revealed that confluent injury of liver cells with intracytoplasmic acidophilic and ballooning change and nuclear pyknosis. The periportal area damages of liver were more severe in mice fed with 100 μg than in mice fed with 10 μg of Gh-rTDH (Figure 19 E and F). Otherwise, the similar findings could be noted in each mice group received liver biopsy (each group n=3). Therefore, these findings demonstrated that Gh-rTDH drained from the portal vein system and made injuries over periportal areas.

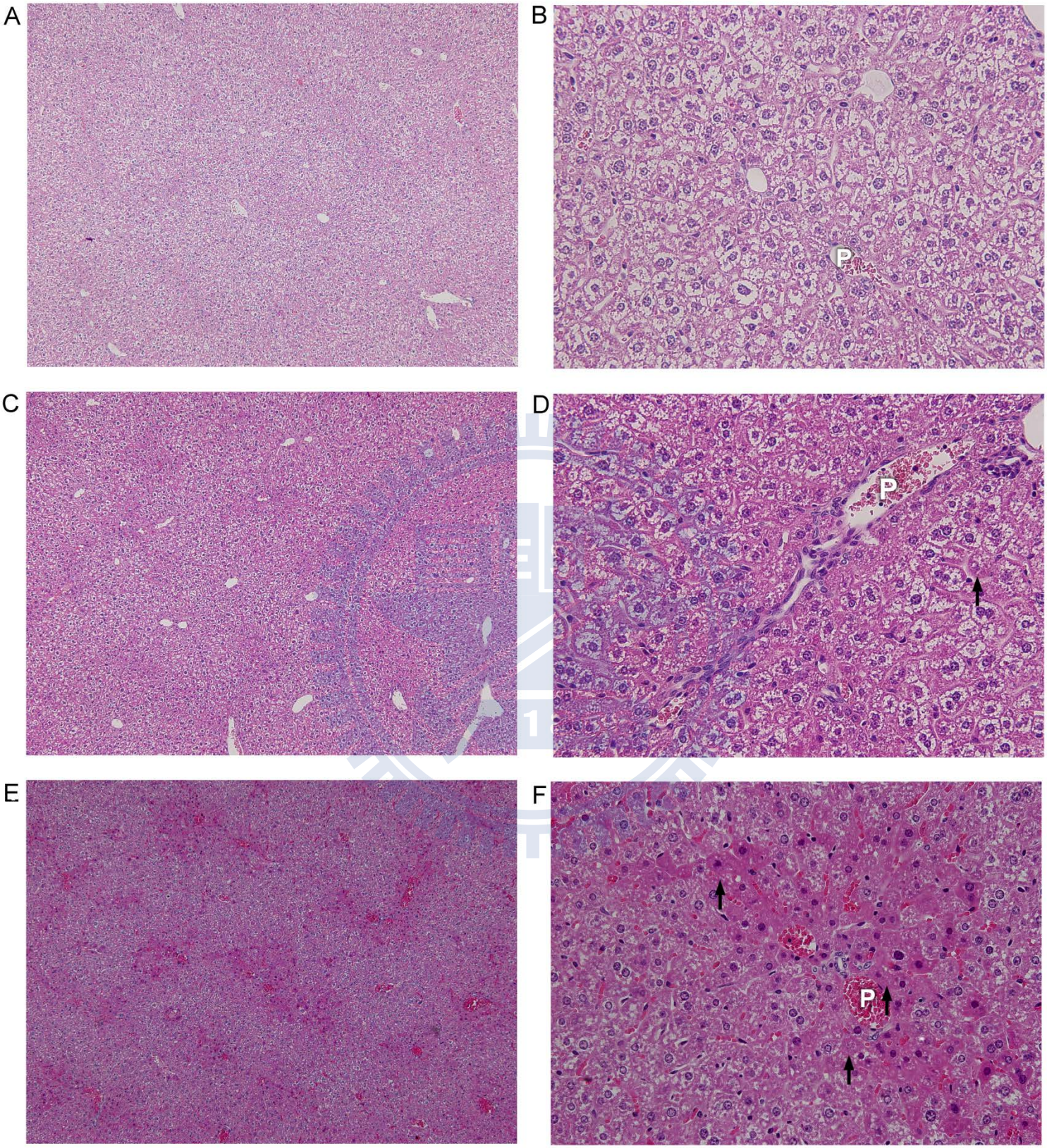

Figure 19 Liver biopsy demonstrate that the damages located in the periportal area of

liver. The pathological images of liver parenchyma which obtained from liver biopsy in mice, were observed by microscopy at low power magnification -100X (A)(C)(E) and at high power magnification- 400X (B)(D)(F). In the mice fed with PBS (control groups), (A) the parenchyma were homogenous and health, (B) liver cells around portal vein were not damaged. In the mice fed with 10 μg of Gh-rTDH, (C) the parenchyma were mild congestive over the periportal areas and (D) the spotty damages could be noted in liver cells around the portal vein. In the mice fed with 100 μg of Gh-rTDH, (E) the parenchyma were severe congestive with hemorrhage around the periportal areas and (F) most of the liver cells around the portal vein were damaged, these cells revealed that confluent injury of liver cells with intracytoplasmic acidophilic and ballooning change and nuclear pyknosis. Above all, these images demonstrated that the Gh-rTDH was absorbed by intestine and caused secondary injury to the liver via venous return of portal system.

P: portal vein, Arrows: the damaged liver cells

3.35 Decrease and recovery in metabolism of livers in living animals evaluated by PET/CT scan

In the mice fed with Gh-rTDH, the levels of ^{18}F-FDG uptake were decreased than in those fed with PBS. The decreases were dose- and time dependent. The red

color light in merge images indicated that ^{18}F-FDG was uptake by cells. General lower level of ^{18}F-FDG uptake could be noted in mice fed with higher dosage with Gh-rTDH and shock state complicated with multiple organ failure was highly suspected (Figure 20A-I). The level of ^{18}F-FDG uptake in liver was further surveyed in cross section images. In our study, each mouse had three series of images including CT, PET and merge of CT and PET after receiving PET/CT scan (Figure 21A). We found that in the mouse fed with Gh-rTDH, their ^{18}F-FDG uptake in liver were obviously fewer than in mouse fed with PBS, and their decreases were in proportion to the dosages of Gh-rTDH (Figure 21B). Moreover, we also noted that the ratios of liver/muscle ^{18}F-FDG uptake level were obviously decreased in the 8th hour after feeding with Gh-rTDH and the severity was dose-dependent. In addition, the ratios of liver/muscle ^{18}F-FDG uptake level recovered to the normal range and even crossed the normal range in the 72th and 168th hour after feeding with Gh-rTDH, respectively. These results indicated that the metabolisms of livers exposed to Gh-rTDH were initially decreased and the recovery continued at least for one week after single exposure of toxin (Figure 21C). The severities of organ damages were provided by ^{18}F-FDG PET/CT scan in the mice fed with Gh-rTDH for 8 hours. Intestine and liver were both the major organs damaged by feeding with different dosages of Gh-rTDH and the damages were also dose-dependent (Figure 22A-C).

A

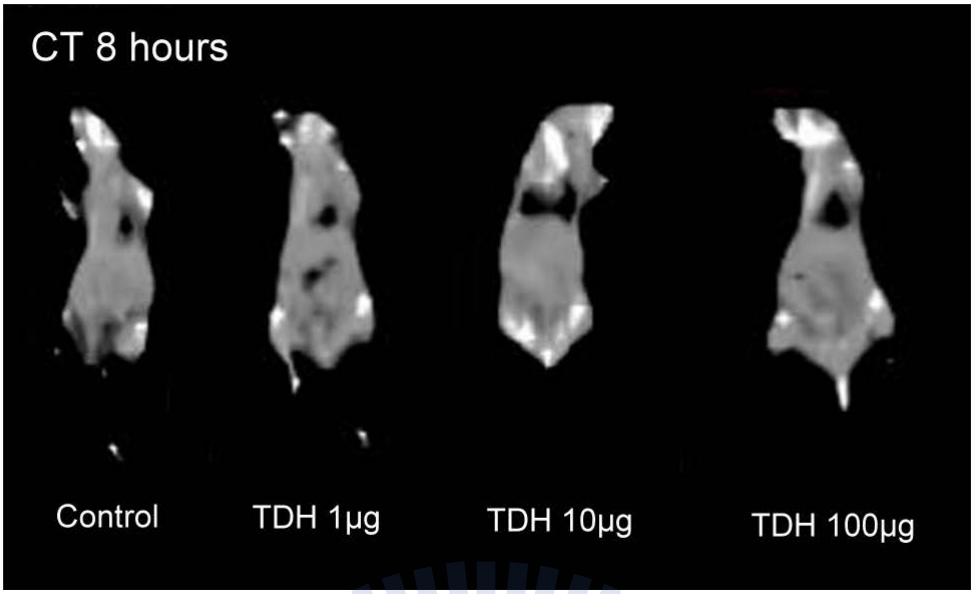
CT 8 hours
Control
TDH 1μg
TDH 10μg
TDH 100μg

B

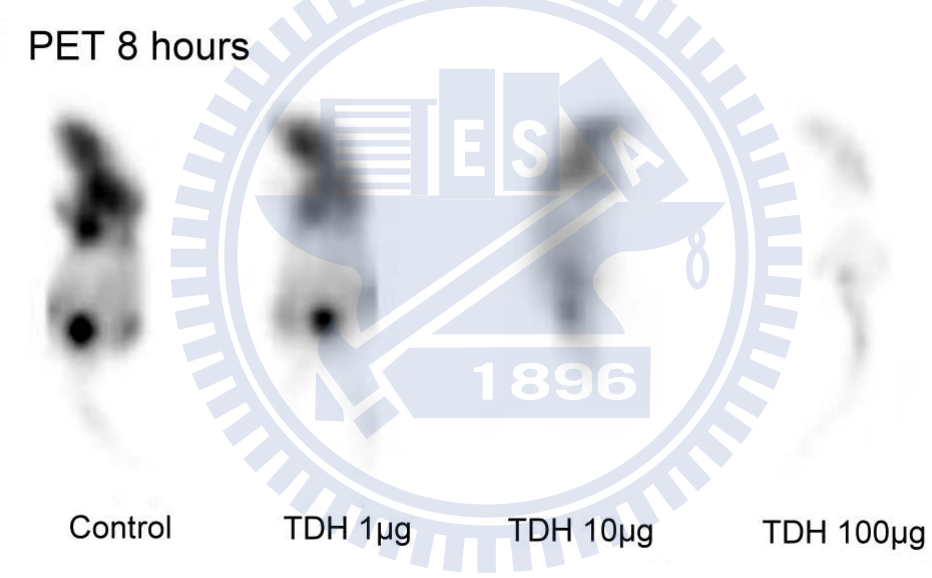
PET 8 hours
Control
TDH 1μg
TDH 10μg
TDH 100μg

C

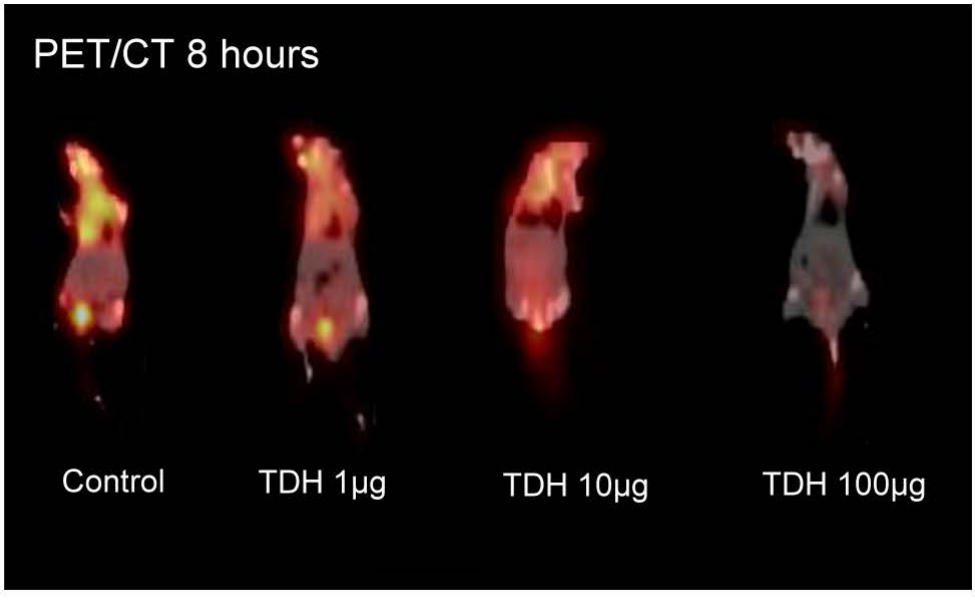
PET/CT 8 hours
Control
TDH 1μg
TDH 10μg
TDH 100μg

D

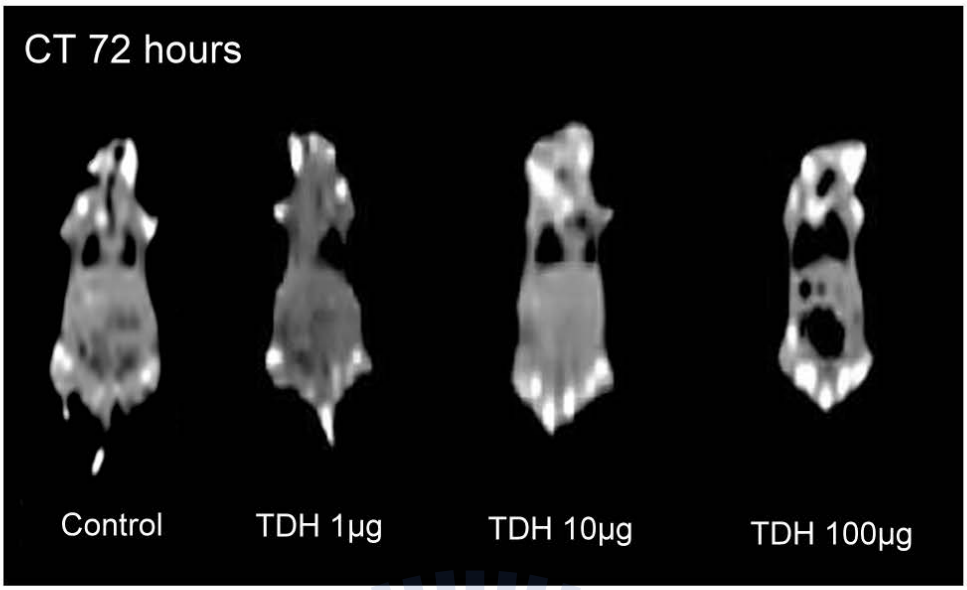
CT 72 hours
Control
TDH 1μg
TDH 10μg
TDH 100μg

E

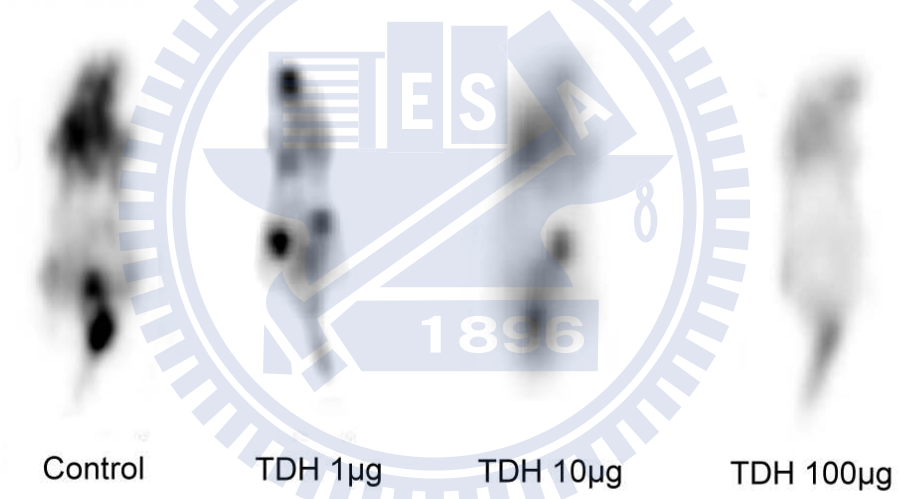
PET 72 hours
Control
TDH 1μg
TDH 10μg
TDH 100μg

F

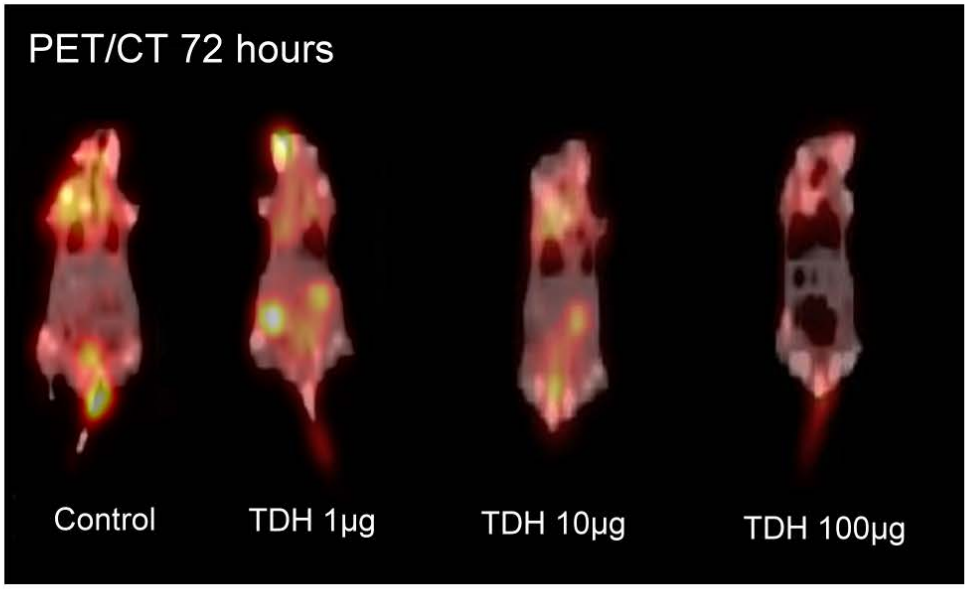
PET/CT 72 hours
Control
TDH 1μg
TDH 10μg
TDH 100μg

G

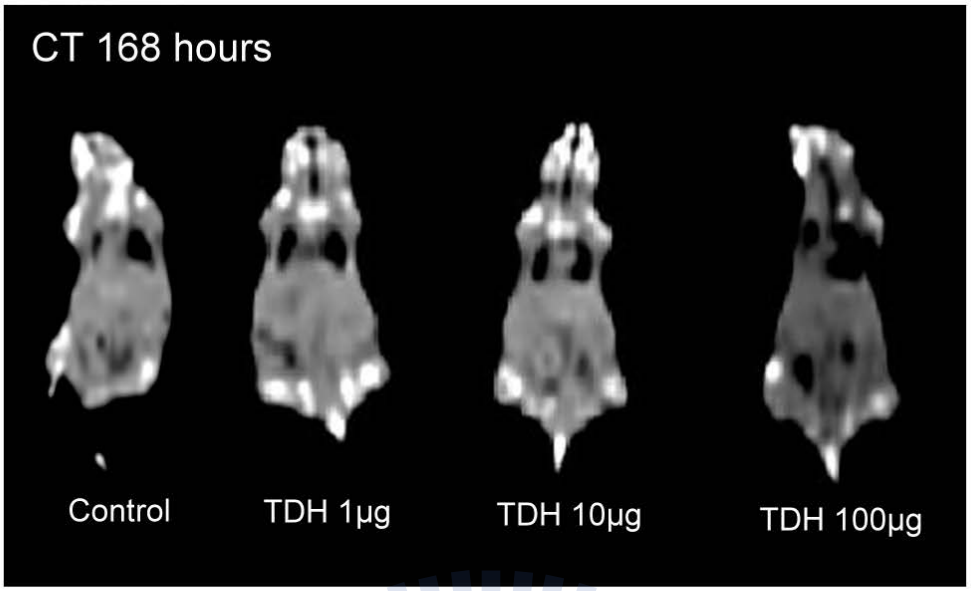
CT 168 hours
Control
TDH 1μg
TDH 10μg
TDH 100μg

H

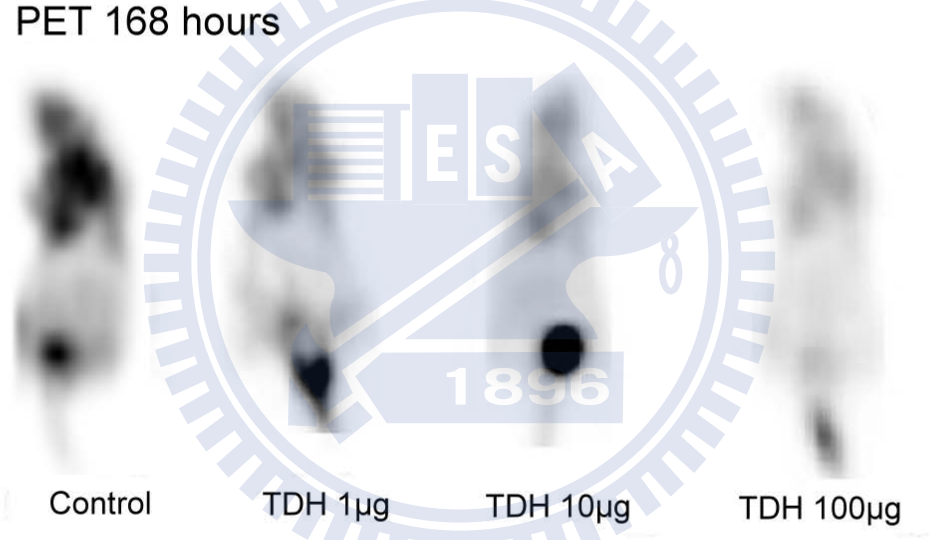
PET 168 hours
Control
TDH 1μg
TDH 10μg
TDH 100μg

I

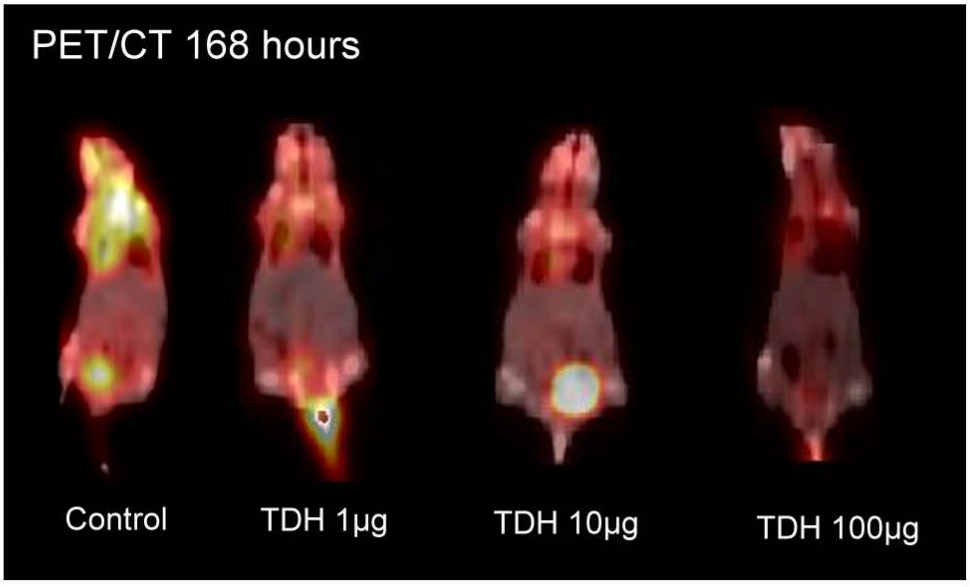
PET/CT 168 hours
Control
TDH 1μg
TDH 10μg
TDH 100μg

Figure 20 Low levels of ^{18}F-FDG uptake could be noted in mice fed with different dosages of Gh-rTDH and shock state was noted. All mice had 3 series of images including (A)(D)(G) CT, (B)(E)(H) PET and (C)(F)(I) merge of CT and PET. In the 8th (A-C), 72th (D-F) and 168th (G-I) hours after feeding with Gh-rTDH, the general uptake of ^{18}F-FDG were all decreased in proportion to the dosages of Gh-rTDH. Mice in control group were fed with PBS.

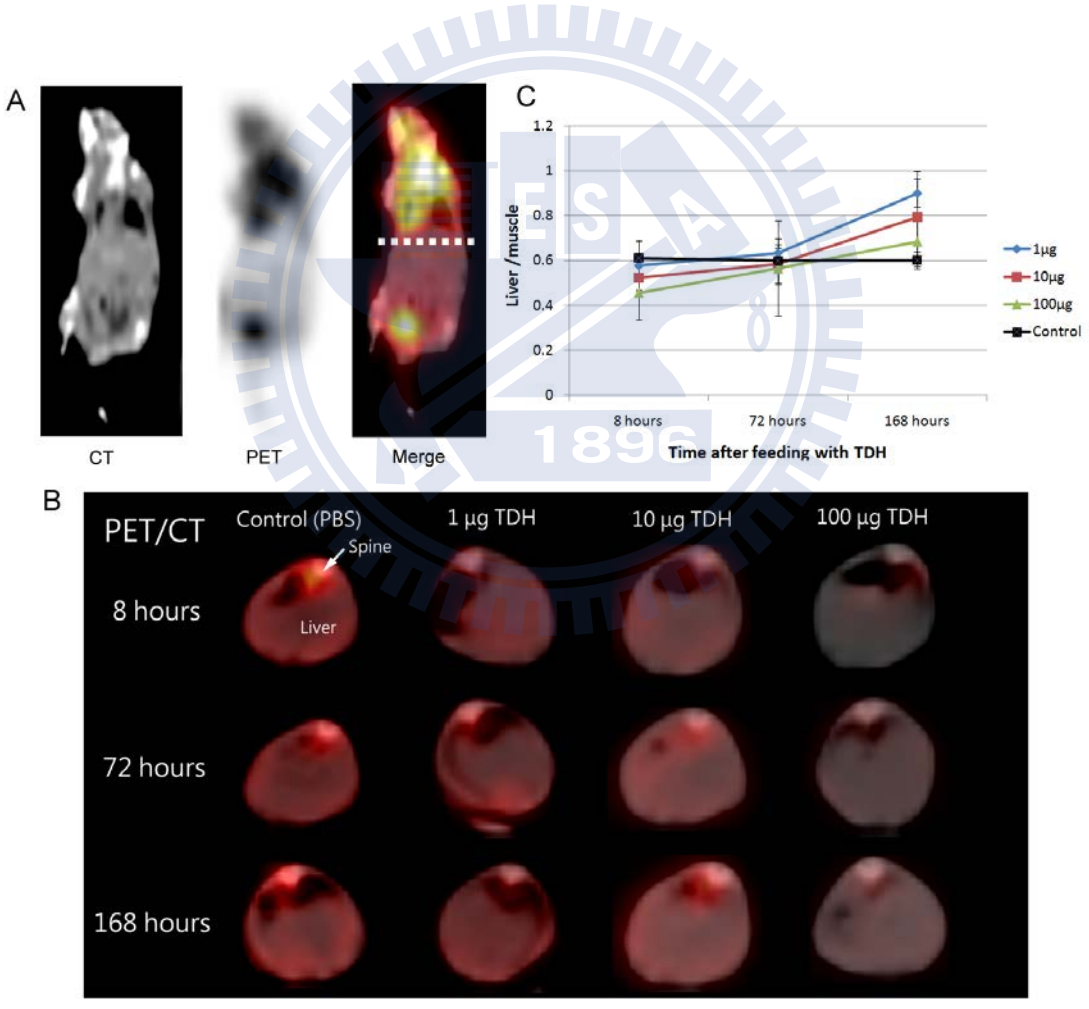

Figure 21 ^{18}F-FDG PET/CT scan for mice treated with Gh-rTDH**.** Mice were administrated for 0.07 mCi ^{18}F-FDG by tail vein injection and images taking were

performed 1 hour later. (A) All mice had 3 series of images including CT, PET and merge of CT and PET. The location of liver was labeled as a dotted line where the cross section images were obtained. (B) These images were cross section of livers. In the 8^{th}, 72^{th} and 168^{th} hours after feeding with Gh-rTDH, the uptake of ^{18}F-FDG in livers were all decreased in proportion to the dosages of Gh-rTDH. (C) The ^{18}F-FDG uptake value was calculated using ROI in each mouse (total n=60); the ROIs of liver and muscle were recorded for semi-quantification in the groups fed with PBS (control), 1 μg, 10 μg and 100 μg of Gh-rTDH (each group n=15, and each group were equally divided into 3 groups in different time points: 8^{th} (n=5), 72^{th} (n=5) and 168^{th} (n=5) hours). The ratios of liver/muscle ^{18}F-FDG uptake level were much fewer in mice fed with Gh-rTDH than in those fed with PBS within the initial 8 hour. Moreover, the levels returned and crossed to the normal range in the 72^{th} hour and 168^{th} hour, respectively.

PET/CT scan in evaluating multiple organs injury after exposure to TDH for 8 hours

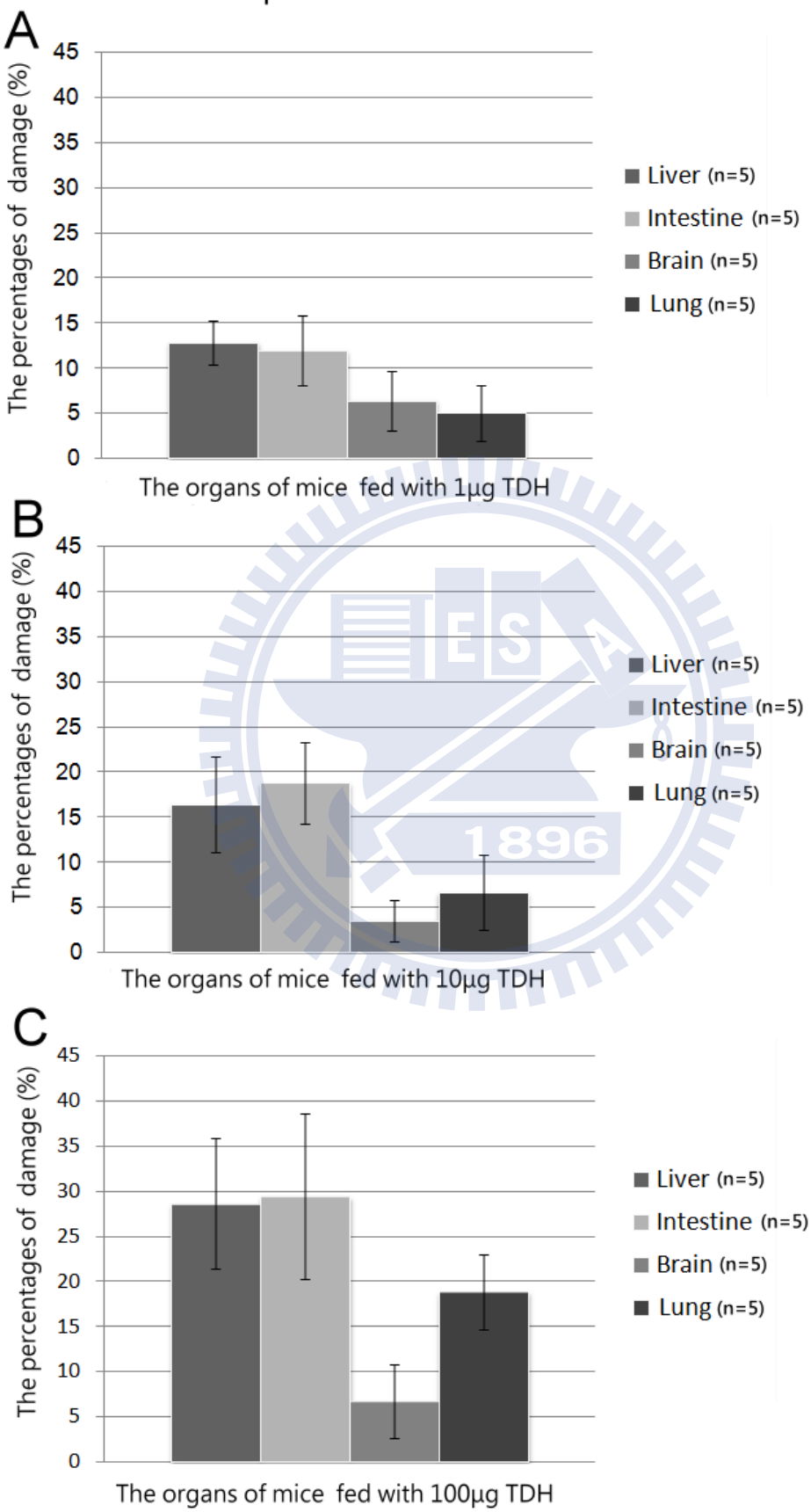

Figure 22 In the mice fed with Gh-rTDH for 8 hours, they were administrated for 0.07 mCi ^{18}F-FDG by tail vein injection and images taking were performed. The severities of organ damages were provided by ^{18}F-FDG PET/CT scan. Intestine and liver were both the major organs damaged by feeding with (A) 1 μg; (B) 10 μg and (C) 100 μg of Gh-rTDH and the damages were also dose-dependent.

3.4 Fiber form of Gh-rTDH did not cause *in vivo and in vitro* hepatotoxicity

The fiber form of Gh-rTDH did not have hemolytic activity in our study. Cell morphology did not change after exposure to fiber form of Gh-rTDH for 24 hours and MTT assay revealed that the cytoviability of FL83B cells also did not decrease after treating fiber form of Gh-rTDH in different dosage and treating durations. In mice fed with fiber form of Gh-rTDH their liver function tests were normal (Figure 23A-E) and liver biopsy were negative finding (Figure 24A-C).

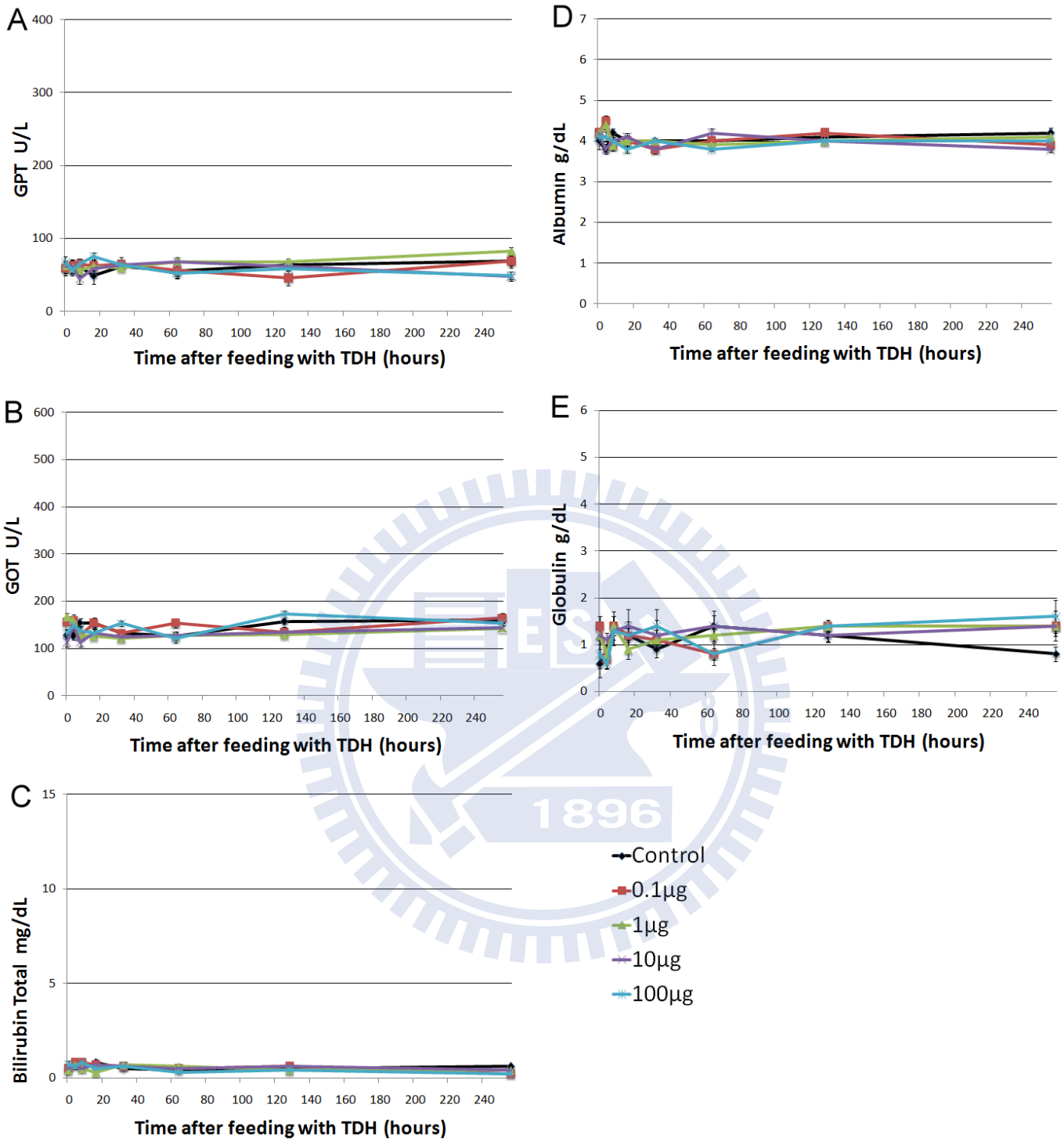

Figure 23 The levels of liver functions were normal in the serum of mice after single administration of fiber form of Gh-rTDH. Six-week-old female BALB\c were respectively fed with four different dosages of fiber form of Gh-rTDH (0.1 μg, 1 μg,

10 μg and 100 μg) and control group were fed with PBS (each group n=5). The levels of (A) GPT and (B) GOT did not elevate. (C) Hyperbilirubinemia and (D) hypoalbumenia were not occurred. (E) The levels of globulin were not increased after exposure to Gh-rTDH.

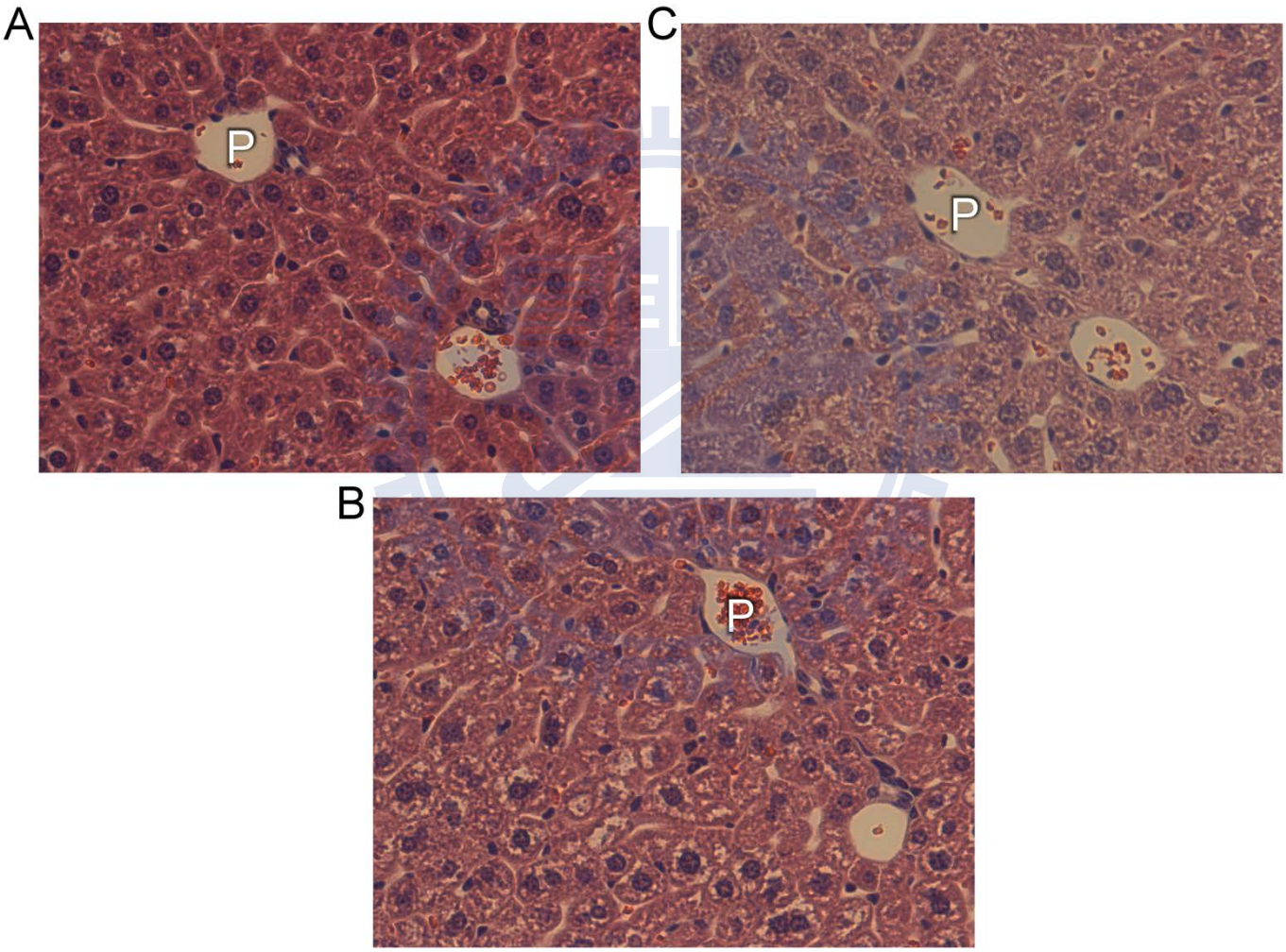

Figure 24 The pathological images of liver parenchyma which obtained from liver biopsy in mice were observed by microscopy at 200X magnification. In the mice fed with PBS (control groups), (A) the parenchyma were homogenous and health and

liver cells around portal vein were not damaged. Similar finding were noted in the mice fed with (B) 10 and (C) 100 μg of fiber form of Gh-rTDH. Above all, fiver form of Gh-rTDH did not cause periportal area damages in liver. **P: portal vein**

3.5 *G. hollisae* and *E. coli*-TOPO-tdh but not *E. coli*-TOPO causes *in vivo* hepatotoxicity

3.51 Liver damages in vivo were induced by G. hollisae and E. coli-TOPO-tdh.

In the control group, the GOT and GPT level did not elevate after feeding them with a single dosage of *E. coli*-TOPO (Figure 25). However, in the group fed with *G. hollisae* (Figure 26) and *E. coli-TOPO-tdh* (Figure 27), the mean GOT and GPT levels were obviously elevated and the highest levels could both be respectively found in the 16th hour and 8th hour after feeding with bacteria. Higher concentrations of bacteria are clearly associated with higher levels of GOT and GPT, which clinically indicate more severe liver injury in mice. Acute hemolytic status, poor functions of albumin synthesis and more triggered immune system could be noted in the mice fed with *G. hollisae* and *E. coli*-TOPO-*tdh*. These patterns were similar with mice directly fed with toxin (Gh-rTDH).

3.52 Decrease and recovery in metabolism of livers in mice evaluated by ^{18}F-FDG

PET/CT scan.

We found that in the mice fed with *G. hollisae* (Figure 28) and *E. coli*-TOPO-*tdh* (Figure 29), ^{18}F-FDG uptakes in their livers were obviously fewer than in mice fed with *E. coli*-TOPO (Figure 30), and their decreases were in proportion to the amount of bacteria. Moreover, we also noted that the ratios of liver/muscle ^{18}F-FDG uptake levels decreased in the 8th hour after feeding with *G. hollisae* and *E. coli*-TOPO-*tdh*. Among them, the ratios of liver/muscle ^{18}F-FDG uptake levels recovered in the 72th and 168th hour, respectively (Figure 31A and B). Moreover, *E. coli*-TOPO did not cause significant liver injuries (Figure 31C).

3.53 Liver biopsy demonstrates that the damages were located in the periportal area of the liver.

In mice fed with *G. hollisae*, the liver biopsy demonstrated obvious cell damages over the periportal areas (Figure 32A). Spotty liver cell damages around the portal vein were noted in mice fed with *E. coli*-TOPO-*tdh* (Figure 32B). Finally, in the mice fed with *E. coli*-TOPO, there was no pathological damage in liver parenchyma (Figure 32C)

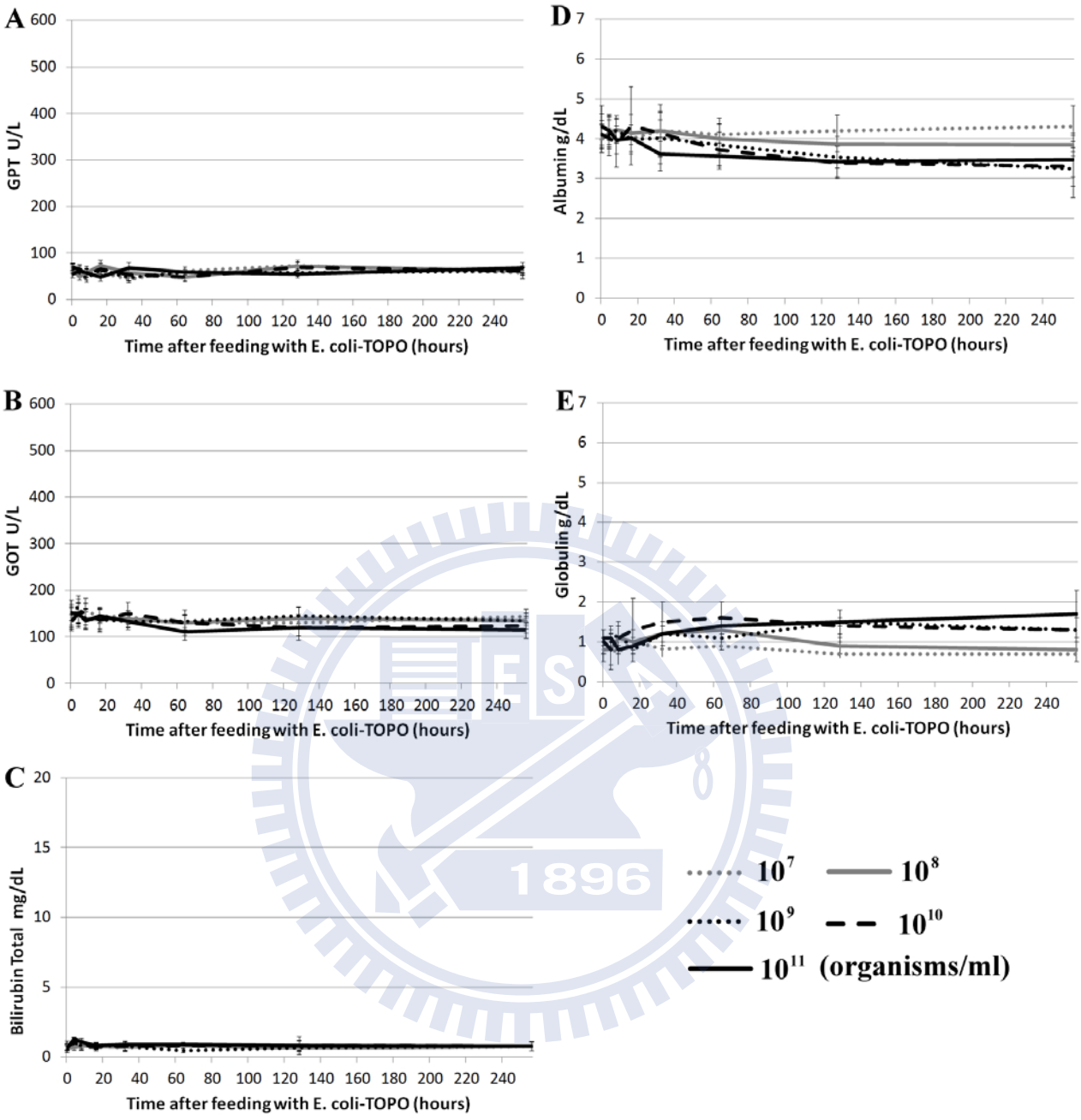

Figure 25 *E. coli*-TOPO did not cause abnormal liver functions. In the control group, the GOT and GPT level did not elevate after feeding them with a single dosage of *E. coli*-TOPO.

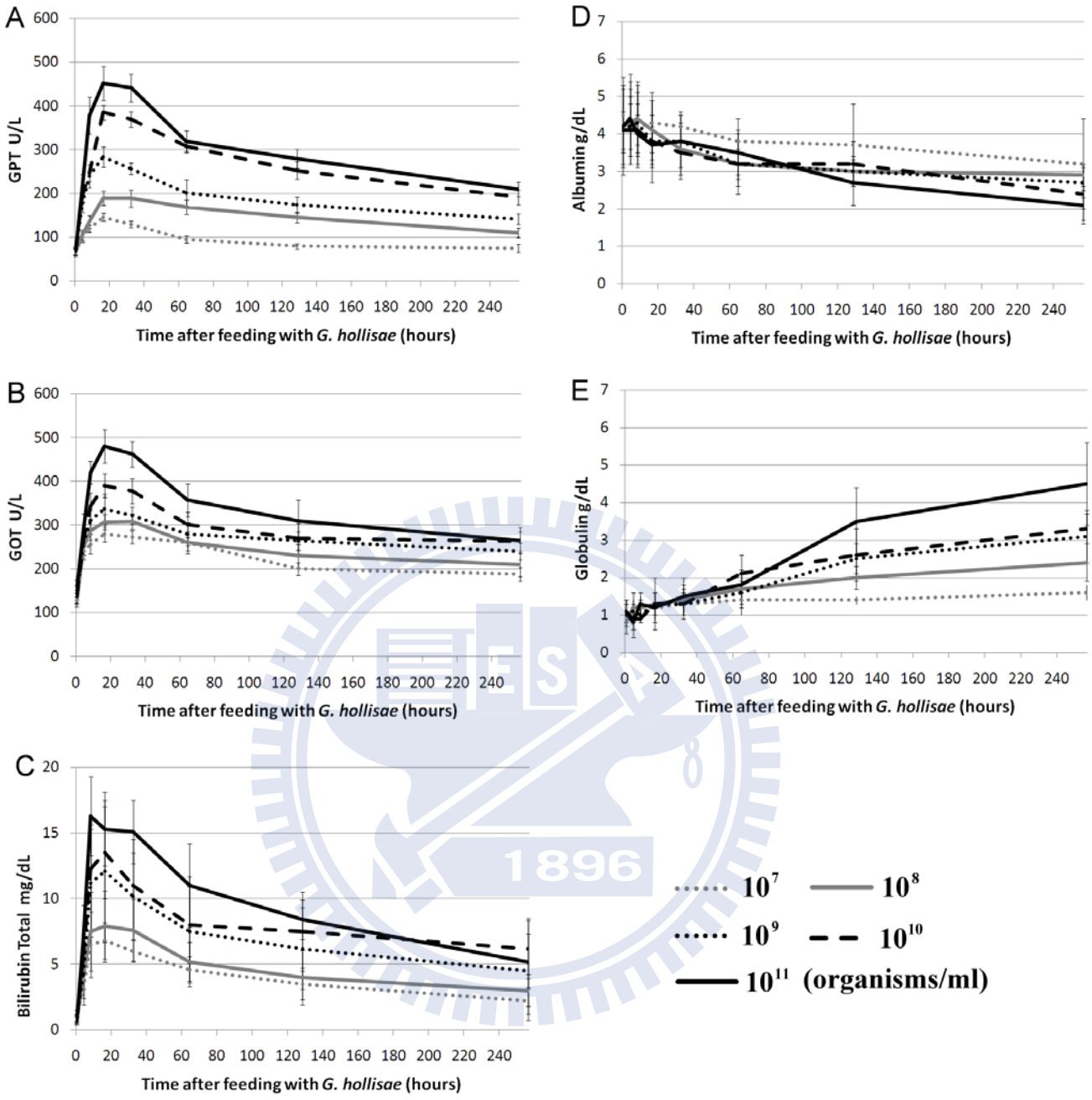

Figure 26 Acute liver injury could be noted in mice fed with *G. hollisae.* GOT/GPT levels were obviously elevated and the highest levels could both be respectively found in the 16th hour and 8th hour after feeding with bacteria.

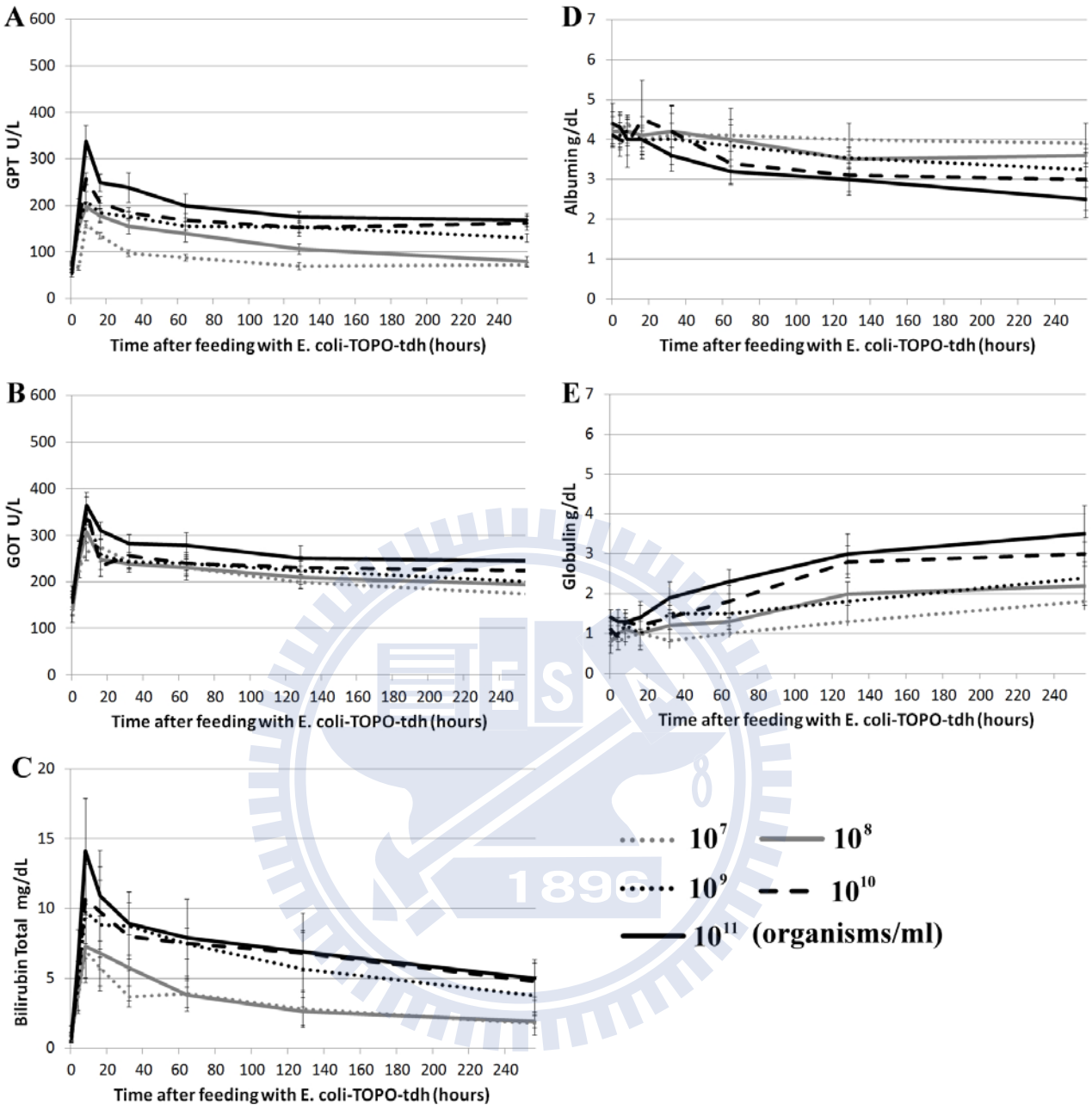

Figure 27 Acute liver injury could be noted in mice fed with *E. coli-TOPO-tdh.* GOT/GPT levels were also obviously elevated and the highest levels could both be respectively found in the 16th hour and 8th hour after feeding with bacteria. This pattern was similar with those fed with *G. hollisae.*

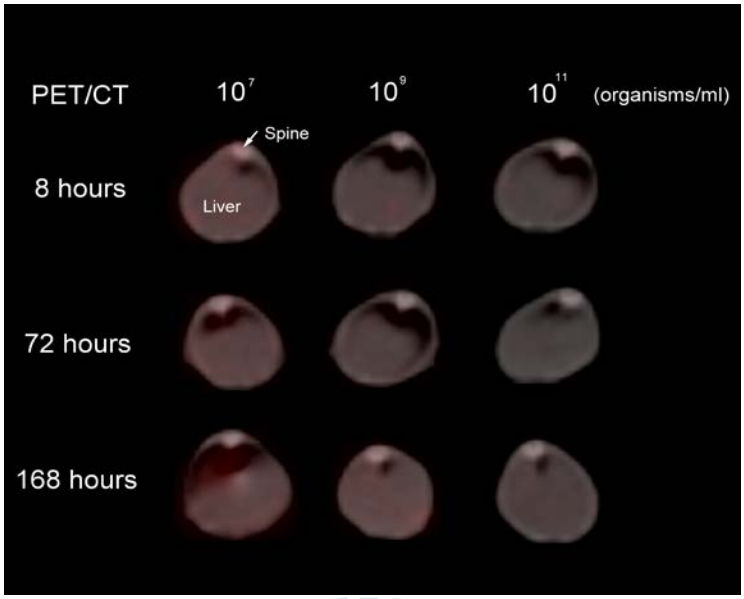

Figure 28 ^{18}F-FDG uptakes in livers were obviously decreased in the mice fed with *G. hollisae*. The decreases were in proportion to the amount of bacteria.

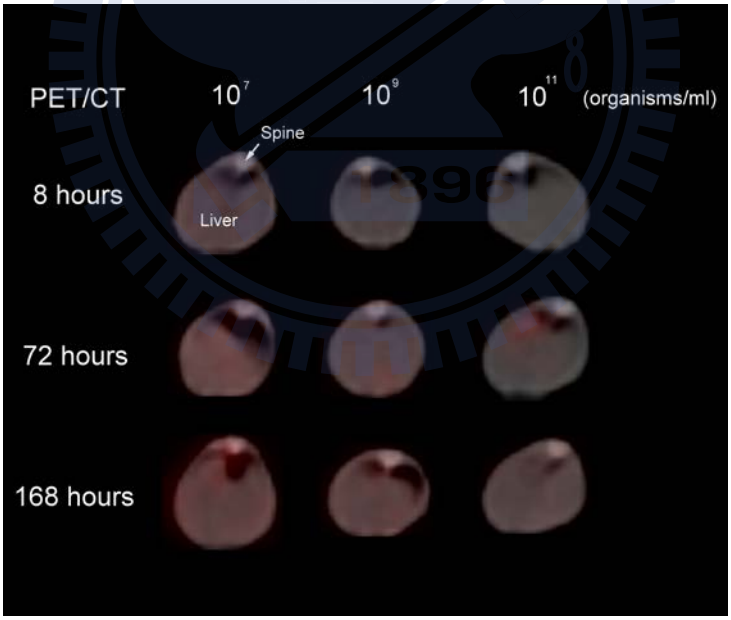

Figure 29 ^{18}F-FDG uptakes in livers were obviously decreased in the mice fed with *E. coli-TOPO-tdh.* The decreases were in proportion to the amount of bacteria.

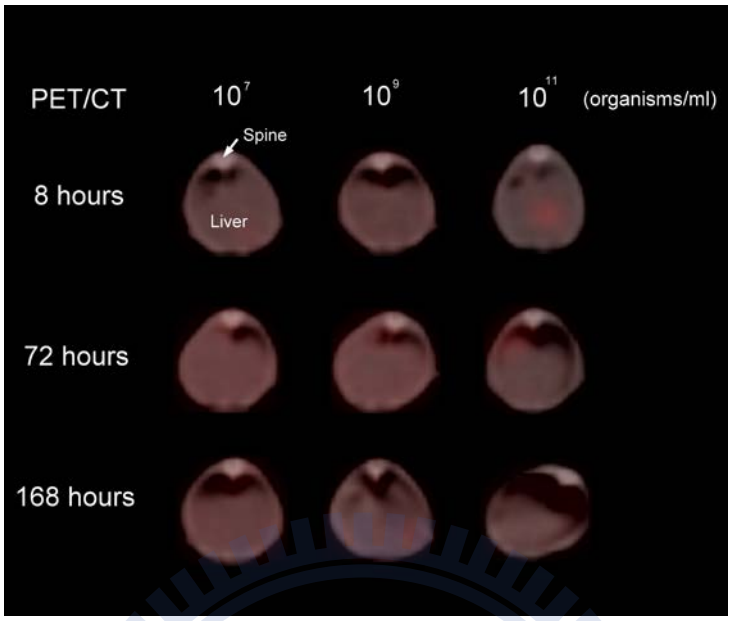

Figure 30 *E. coli*-TOPO did not cause obvious liver injury. The uptakes of ^{18}F-FDG were not decreased.

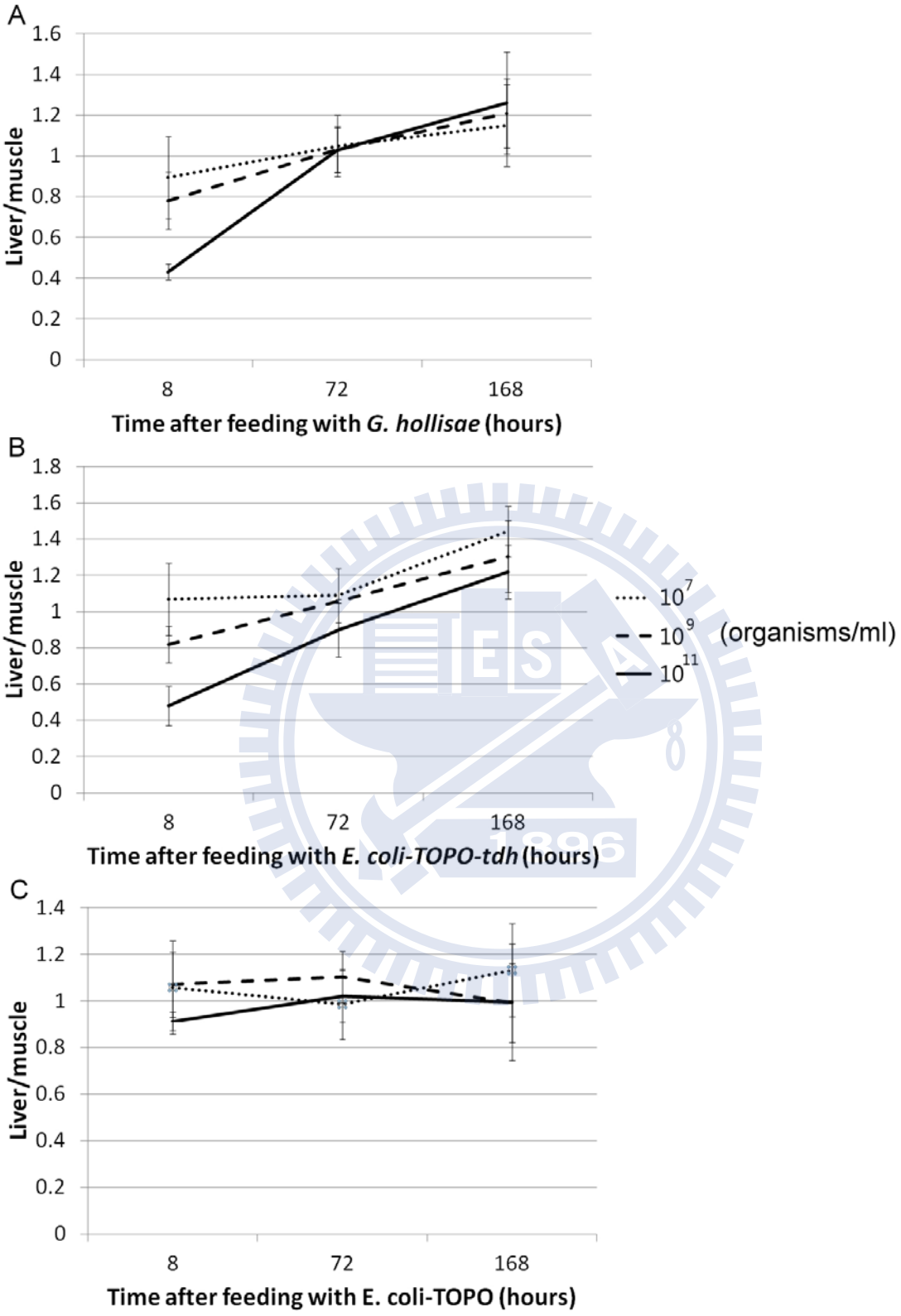

Figure 31 The ratios of liver/muscle ^{18}F-FDG uptake levels in mice fed with bacteria.

The ratios of liver/muscle ^{18}F-FDG uptake levels recovered in the 72th and 168th hour,

respectively (A and B). Moreover, *E. coli*-TOPO did not cause significant liver injuries (C).

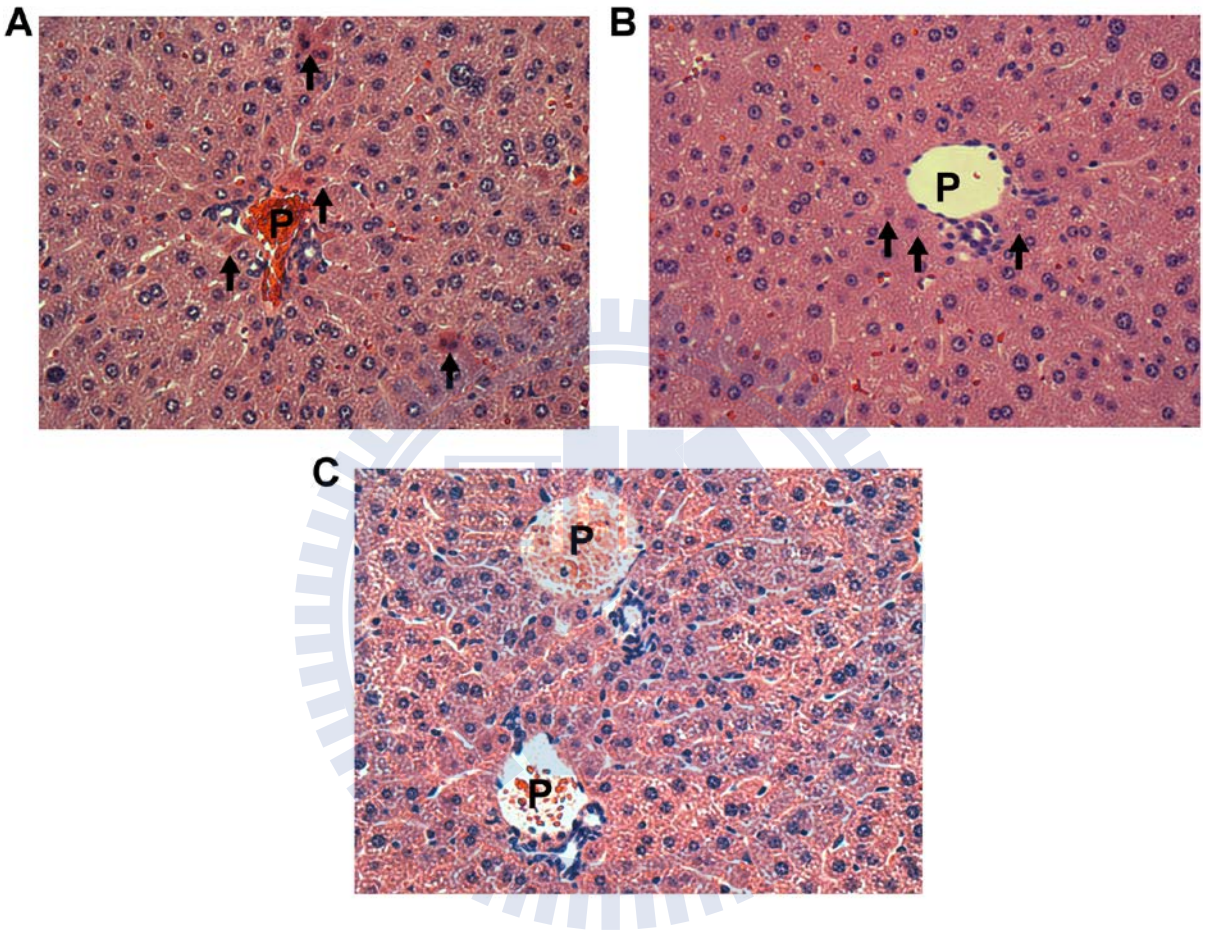

Figure 32 Liver biopsy (tissue harvested at the time of animal sacrifice) following bacterial infection. In mice fed with *G. hollisae,* the liver biopsy demonstrated obvious cell damages over the periportal areas (A). Spotty liver cell damages around the portal vein were noted in mice fed with *E. coli*-TOPO-*tdh* (B). Finally, in the mice fed with *E. coli*-TOPO, there was no pathological damage in liver parenchyma (C)

Chapter 4 Discussion

In this study, liver cells were firstly treated with *G. hollisae* TDH and the *in vitro* hepatotoxicity was demonstrated by direst observation and MTT assay. The hepatotoxicity caused by Gh-TDH was both dose- and time-dependent. Very low concentration of TDH (> 10^{-6} μg/ml) damaged the liver cells. We also noted that the MTT assays yielded a similar pattern over 12, 16, 24, and 48 hr under different toxin concentrations. One possible explanation is that when the concentration of toxin increased, cells were not only killed by this toxin but also probably suffered cell division suppression. Therefore, when we prolonged the treatment durations, the number of surviving cells did not clearly differ between the 4 time points. Naim et al. reported that *V. parahaemolyticus* TDH caused Rat-1 cells injury and the TDH might induce cytotoxicity by acting inside the cells.(27) In our study, we noted that the Gh-rTDH-FITC invaded inside of liver cells via binding around the margin of cell and further located in their nucleus in short time. Therefore, the destructions caused by *G. hollisae* TDH were quite quick and lethal in liver cells.

Morros et al. firstly reported a patient suffered *G. hollisae* infection and presented with liver cirrhosis and hepatic encephalopathy in 1982.(28) Some previous studies demonstrated that the symptoms of patients with *Vibrio* species infections could be more severe in those who had history of impairment liver functions.(1, 14)

However, the evidence of hepatotoxicity caused by *G. hollisae* TDH had never been provided. In this study, we found that the GOT and GPT levels of mice fed with Gh-rTDH were obviously increased and acute liver injury were highly suspected. Muscle injury was not favored as the major reason for the elevation of GOT/GPT, as a ^{18}F-FDG PET/CT scan did not show muscle injury. Moreover, the liver biopsy revealed that the periportal areas of liver were damaged and their severity associated with the dosage of Gh-rTDH. The functions of periportal area in liver were well known as oxidative energy metabolism of fatty and amino acids, glucose release and glycogen formation, ammonia detoxification, protective metabolism, and the synthesis of albumin.(29-31) Therefore, mice with periportal area injury caused by Gh-rTDH might also suffer some complications including malnutrition, protective system destruction, hepatic encephalopathy and hypoalbumenia. Clinically, the hypoalbumenia could be induced by decreased (hepatic) production or increased loss (gut tract loss). The result of hypoalbumenia in this study might be influenced by both mechanisms. The globulin levels also increased as the protective systems of the livers were damaged and the toxin triggered their immune systems in the circulation. Overall, the evidence of hypoalbumenia could be provided in our mice fed with Gh-rTDH and in whom their globulin levels also increased because of their protective systems in liver were destructed and the toxin triggered immune system in circulation.

TDH was well known as having a strong hemolytic activity *in vitro*.(14, 23, 32, 33) However, the *in vivo* hemolysis caused by TDH had not been well provided. The acute hemolytic status *in vivo* results in acute anemia, which would exacerbate tissue hypoxia and organ hypoperfusion. Therefore, septicemia caused by *Vibrio* species with the *tdh* gene might be more critical than that caused by the *Vibrio* species without the *tdh* gene. Clinically, the hepatotoxicity might be caused via hemolysis. However, the pathological findings revealed that the hepatic injury was mainly located at the periportal areas, and the injury was not diffused. It is suspected that the major etiology is toxin absorption and injury to the liver via the venous return of the portal system.

Clinical PET/CT scan had been reported as an excellent tool to survey tumor and organ metabolism in small animals.(34) Damages of liver caused by Gh-rTDH could be demonstrated by blood withdrawal and liver biopsy. However, the conditions of recovery and organ metabolism in living animals were difficult to be analyzed. Therefore, ^{18}F-FDG PET/CT scan was performed in our assessment. We noted that the uptake of ^{18}F-FDG in the livers decreased in proportion to the feeding dosages of Gh-rTDH, which indicated that the damages of livers in living animals were dose-dependent. After single exposure to Gh-rTDH, the uptake of ^{18}F-FDG gradually increased in trend. We suggested that the livers could finally reconstruct from the

destruction of Gh-rTDH exposure and these liver cells undergone repair and proliferation via increasing the uptake of glucose, which was well known as an unavoidable material in metabolism. The metabolism of glucose in the livers damaged by Gh-rTDH almost recovered to normal range in the 72th hours after exposure to TDH. Furthermore, the metabolism of glucose crossed the normal range in the 168th hours after exposure to Gh-rTDH, and the recovery was more predominant in the mice feeding with low dosage than in those feeding with high dosage of Gh-rTDH. The level of uptake crossed the normal range pointed out that the metabolism of glucose were truly exuberant in these damaged livers and indicated a stage of strong recovery. Also, according to our finding of liver biopsy, the construction might mainly located in the periportal area where had been well labeled as a major location of glucose and amino acid metabolism.(29-31) Therefore, the construction in periportal area might contribute the high level of ^{18}F-FDG intake in the liver during recovery stage. Overall, this finding might provide strong evidence which indicated that the reconstruction of liver continued at least for one week after single exposure of Gh-rTDH and the damaged liver provide an ability to recover from the Gh-rTDH related injury even when they exposed to a massive dosage of Gh-rTDH. Consistent with this observation is the finding that differential hepatotoxicity could be detected when mice were treated with different amounts of *G. hollisae and E. coli*-TOPO-*tdh*

but were free from hepatotoxicity with *E. coli*-TOPO. The ^{18}F-FDG PET/CT results of the animal infection models showed that the severity of the liver injury was notably similar in mice treated with 100 μg of Gh-TDH and in mice treated with 10^{10} organisms of *G. hollisae*. Therefore, we suspected that 10^{8} organisms of *G. hollisae* might produce 1 μg of TDH and cause liver injury *in vivo*. The results clearly demonstrate the *in vivo* hepatotoxicity of the *Gh-tdh* gene product.

In conclusion, *G. hollisae* TDH is reported as having *in vitro* and *in vivo* hepatotoxicity in our study. *G. hollisae* TDH damaged the liver in living animals and mainly attacked the periportal area, which is associated with the synthesis of albumin and the metabolism of glucose. Most importantly, the ^{18}F-FDG PET/CT scan revealed evidence that the reconstruction of the liver continued at least for one week after a single exposure of *G. hollisae* TDH. Furthermore, the damaged liver was shown to have an adequate ability to recover.

Chapter 5 Conclusion and future perspectives

In this study, we demonstrated that TDH from *G. hollisae* cause *in vitro* and *in vivo* hepatotoxicity. However, the relationship between chronic liver diseases (ie, chronic hepatitis, liver cirrhosis and hepatocellular carcinoma) and TDH infection had never been further analyzed. We aim to analyze this topic in the future.

5.1 Analyze the relationships between chronic liver diseases and TDH

The toxin effects of TDH had been identified from a variety of *Vibrio* species, including *V. cholera* non-O1, *V. parahaemolyticus*, *V. mimicus*, *V. alginolyticus*, and *G. hollisae*.[18-22] According to our previous findings, *G. hollisae* TDH caused acute liver injury and abnormal liver functions including elevated levels of GOT/GPT, hyperbilirubinemia and hypoalbumenia in mice. Liver biopsy also revealed that TDH mainly damaged the periportal areas of liver and resulted in protective system impairment. High levels of globulin in mice exposure to TDH also demonstrated that their immune systems were triggered by feeding with TDH. Clinically, the overactive immune system might damage the organs of human, especially in liver. It had been well demonstrated that severe or recurrent damages of liver might cause the death of liver cells, interstitial tissue fibrosis and complicated with chronic pathological

changes. Therefore, we highly suspected that the exposure to TDH might associate with the chronic liver diseases in human and we aimed to analyze the relationships in our further works. In Taiwan, seafood is very popular and easily obtained. Economically, seafood is also the major productions in some areas, especially in some countryside of central Taiwan (Figure 33). Previous study reported that *Vibrio* species was more common in oyster and easily causes human diseases.[1] Therefore, we aim to analyze the incidence and prevalence of *Vibrio* species infections in Changhua area (Lu-Kung and Wang Kong), where the oysters are the major seafood productions. In all patients with *Vibrio* species infections, they are divided into two major groups. One is the group with anti-TDH antibody (+) and the other is the group with anti-TDH antibody (-). All of them will be followed up their liver function for 1 year. The exclusion criteria are: patients aged younger than 18 years, alcohol abuse, virus hepatitis, high fat diet habit, past history of drug intoxication, substances abuse and past history of chronic liver disease. Patient with these presentations will be excluded from this study.

Figure 33 Oysters are the major seafood productions of Lu-Kung and Wang Kong in central Taiwan (A-D).

The blood samples are analyzed for their continued liver functions including the levels of GOT, GPT, total bilirubin, albumin and globulin in patients with anti-TDH antibody (+) and anti-TDH antibody (-). The blood samples obtained from the patients with TDH-antibody (-) are suggested to be the control groups in this study. The bilirubin total is further divided into direct and indirect forms and their ratios are also calculated (Assay kits: Aspartate Aminotransferase, Alanine Aminotransferase, Total Bilirubin, Direct Bilirubin, Albumin and Total protein Reagents Beckman Coulter® ;

Supply: Beckman Coulter Synchron CX7 Analyzer). Moreover, each patients will respectively receive blood withdraw after exposure to TDH for 24, 72, 168 and 336 hours. Therefore, their trends of liver functions will be set up and acute livers injury can be demonstrated. The examination of liver ultrasound had been provided to be an excellent tool in analyzing chronic liver disease (ie, liver cirrhosis, liver tumor, chronic hepatitis). In this study, each patient is suggested to receive the examination of liver ultrasound after exposure to TDH for 1, 42, 178 and 365 days in our cooperative EDs. The continued changes of livers will be recorded via taking images (Figure 34). The operators of this examination are all ED attending physicians who had ever received the training course of abdominal sonography at least for 80 hours. In these follow-up patients, liver biopsy is suggested to perform in who presents with chronic liver change. The coagulative function of blood will be surveyed in each patient who will receive biopsy. All samples will be prepared with H&E stain and their pathological images with reports will be provided by the pathology department of Changhua Christian Hospital. Descriptive analyses of independent variables are reported as percentages or mean ±standard deviation (SD). The prevalence of chronic liver diseases in patient with TDH-antibody (+) and TDH-antibody (-) is analyzed for their differences. Factors that may be associated with chronic liver diseases are analyzed by the $\chi 2$ test and Fisher's exact test for the categorical variables and the

Mann-Whitney U test for the continuous variables. A P-value <0.05 was regarded as statistically significant. All statistical analyses were performed on a personal computer with the statistical package SPSS for Windows (Version 15.0, SPSS, Inc., Chicago, IL).

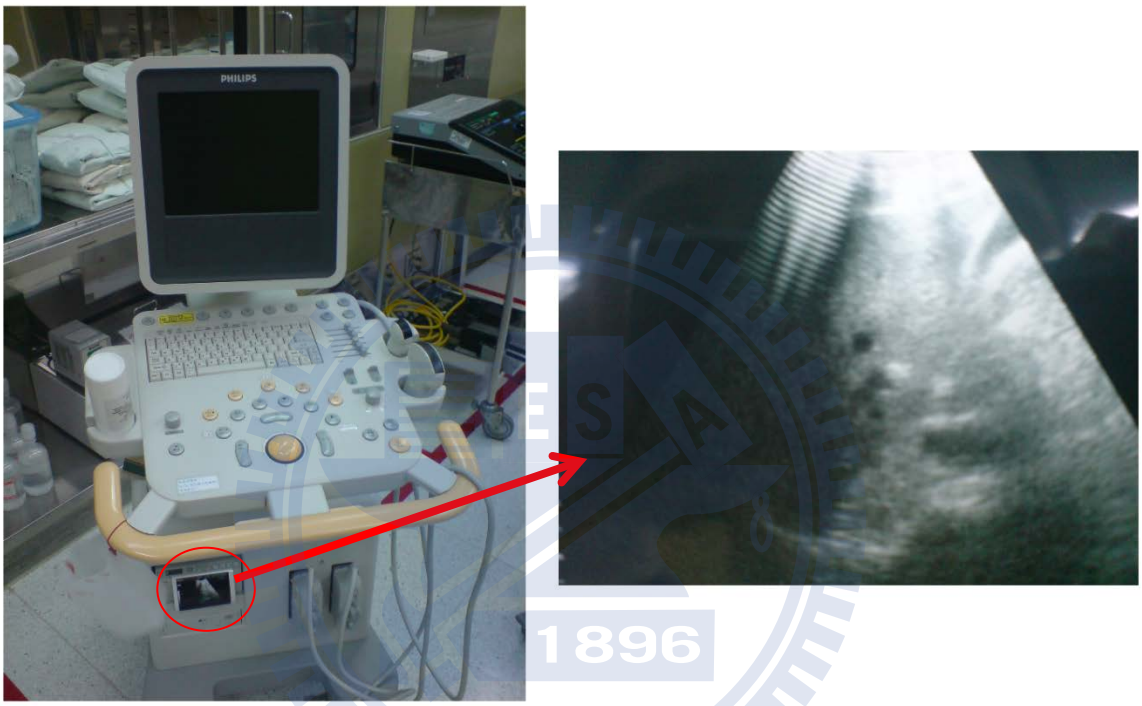

Figure 34 Each patient is suggested to receive the examination of liver ultrasound in our cooperative EDs after exposure to TDH for 1, 42, 178 and 365 days. The continued changes of livers will be recorded via taking images

Chapter 6 References

1 Morris JG,Jr. Cholera and other types of vibriosis: a story of human pandemics and oysters on the half shell. *Clin.Infect.Dis.* 2003; 37: 272-80.

2 Yeung PS, Boor KJ. Epidemiology, pathogenesis, and prevention of foodborne Vibrio parahaemolyticus infections. *Foodborne Pathog.Dis.* 2004; 1: 74-88.

3 Lesmana M, Subekti DS, Tjaniadi P, Simanjuntak CH, Punjabi NH, Campbell JR, Oyofo BA. Spectrum of vibrio species associated with acute diarrhea in North Jakarta, Indonesia. *Diagn.Microbiol.Infect.Dis.* 2002; 43: 91-7.

4 Abbott SL, Janda JM. Severe gastroenteritis associated with Vibrio hollisae infection: report of two cases and review. *Clin.Infect.Dis.* 1994; 18: 310-2.

5 Gras-Rouzet S, Donnio PY, Juguet F, Plessis P, Minet J, Avril JL. First European case of gastroenteritis and bacteremia due to Vibrio hollisae. *Eur.J.Clin.Microbiol.Infect.Dis.* 1996; 15: 864-6.

6 Carnahan AM, Harding J, Watsky D, Hansman S. Identification of Vibrio hollisae associated with severe gastroenteritis after consumption of raw oysters. *J.Clin.Microbiol.* 1994; 32: 1805-6.

7 Cook DW, Oleary P, Hunsucker JC, Sloan EM, Bowers JC, Blodgett RJ, Depaola A. Vibrio vulnificus and Vibrio parahaemolyticus in U.S. retail shell oysters: a national survey from June 1998 to July 1999. *J.Food Prot.* 2002; 65: 79-87.

8 Motes ML, DePaola A, Cook DW, Veazey JE, Hunsucker JC, Garthright WE, Blodgett RJ, Chirtel SJ. Influence of water temperature and salinity on Vibrio vulnificus in Northern Gulf and Atlantic Coast oysters (Crassostrea virginica). *Appl.Environ.Microbiol.* 1998; 64: 1459-65.

9 Daniels NA, MacKinnon L, Bishop R, Altekruse S, Ray B, Hammond RM, Thompson S, Wilson S, Bean NH, Griffin PM, Slutsker L. Vibrio parahaemolyticus infections in the United States, 1973-1998. *J.Infect.Dis.* 2000; 181: 1661-6.

10 Hinestrosa F, Madeira RG, Bourbeau PP. Severe gastroenteritis and hypovolemic shock caused by Grimontia (Vibrio) hollisae infection. *J.Clin.Microbiol.* 2007; 45: 3462-3.

11 Hickman FW, Farmer JJ,3rd, Hollis DG, Fanning GR, Steigerwalt AG, Weaver RE, Brenner DJ. Identification of Vibrio hollisae sp. nov. from patients with diarrhea. *J.Clin.Microbiol.* 1982; 15: 395-401.

12 Thompson FL, Hoste B, Vandemeulebroecke K, Swings J. Reclassification of Vibrio hollisae as Grimontia hollisae gen. nov., comb. nov. *Int.J.Syst.Evol.Microbiol.* 2003; 53: 1615-7.

13 Rank EL, Smith IB, Langer M. Bacteremia caused by Vibrio hollisae. *J.Clin.Microbiol.* 1988; 26: 375-6.

14 Raimondi F, Kao JP, Fiorentini C, Fabbri A, Donelli G, Gasparini N, Rubino A, Fasano A. Enterotoxicity and cytotoxicity of Vibrio parahaemolyticus thermostable direct hemolysin in in vitro systems. *Infect.Immun.* 2000; 68: 3180-5.

15 Park KS, Ono T, Rokuda M, Jang MH, Iida T, Honda T. Cytotoxicity and enterotoxicity of the thermostable direct hemolysin-deletion mutants of Vibrio parahaemolyticus. *Microbiol.Immunol.* 2004; 48: 313-8.

16 Fukui T, Shiraki K, Hamada D, Hara K, Miyata T, Fujiwara S, Mayanagi K, Yanagihara K, Iida T, Fukusaki E, Imanaka T, Honda T, Yanagihara I. Thermostable direct hemolysin of Vibrio parahaemolyticus is a bacterial reversible amyloid toxin. *Biochemistry* 2005; 44: 9825-32.

17 Wang YK, Huang SC, Wu YF, Chen YC, Lin YL, Nayak M, Lin YR, Chen WH, Chiu YR, Li TT, Yeh BS, Wu TK. Site-directed mutations of thermostable direct

hemolysin from Grimontia hollisae alter its arrhenius effect and biophysical properties. *Int.J.Biol.Sci.* 2011; 7: 333-46.

18 Nishibuchi M, Janda JM, Ezaki T. The thermostable direct hemolysin gene (tdh) of Vibrio hollisae is dissimilar in prevalence to and phylogenetically distant from the tdh genes of other vibrios: implications in the horizontal transfer of the tdh gene. *Microbiol.Immunol.* 1996; 40: 59-65.

19 Shinoda S, Nakagawa T, Shi L, Bi K, Kanoh Y, Tomochika K, Miyoshi S, Shimada T. Distribution of virulence-associated genes in Vibrio mimicus isolates from clinical and environmental origins. *Microbiol.Immunol.* 2004; 48: 547-51.

20 Cai SH, Wu ZH, Jian JC, Lu YS. Cloning and expression of gene encoding the thermostable direct hemolysin from Vibrio alginolyticus strain HY9901, the causative agent of vibriosis of crimson snapper (Lutjanus erythopterus). *J.Appl.Microbiol.* 2007; 103: 289-96.

21 Yoh M, Honda T, Miwatani T, Tsunasawa S, Sakiyama F. Comparative amino acid sequence analysis of hemolysins produced by Vibrio hollisae and Vibrio parahaemolyticus. *J.Bacteriol.* 1989; 171: 6859-61.

22 Shinoda S. Protein toxins produced by pathogenic vibrios. *J.Nat.Toxins* 1999; 8: 259-69.

23 Nishibuchi M, Doke S, Toizumi S, Umeda T, Yoh M, Miwatani T. Isolation from a coastal fish of Vibrio hollisae capable of producing a hemolysin similar to the thermostable direct hemolysin of Vibrio parahaemolyticus. *Appl.Environ.Microbiol.* 1988; 54: 2144-6.

24 Wang YK, Huang SC, Wu YF, Chen YC, Chen WH, Lin YL, Nayak M, Lin YR, Li TT, Wu TK. Purification, crystallization and preliminary X-ray analysis of a thermostable direct haemolysin from Grimontia hollisae. *Acta Crystallogr.Sect.F.Struct.Biol.Cryst.Commun.* 2011; 67: 224-7.

25 Anspach FB. Endotoxin removal by affinity sorbents. *J.Biochem.Biophys.Methods* 2001; 49: 665-81.

26 Petsch D, Anspach FB. Endotoxin removal from protein solutions. *J.Biotechnol.* 2000; 76: 97-119.

27 Naim R, Yanagihara I, Iida T, Honda T. Vibrio parahaemolyticus thermostable direct hemolysin can induce an apoptotic cell death in Rat-1 cells from inside and outside of the cells. *FEMS Microbiol.Lett.* 2001; 195: 237-44.

28 Morris JG,Jr, Miller HG, Wilson R, Tacket CO, Hollis DG, Hickman FW, Weaver RE, Blake PA. Illness caused by Vibrio damsela and Vibrio hollisae. *Lancet* 1982; 1: 1294-7.

29 Jungermann K. Metabolic zonation of liver parenchyma. *Semin.Liver Dis.* 1988; 8: 329-41.

30 Jungermann K. Functional heterogeneity of periportal and perivenous hepatocytes. *Enzyme* 1986; 35: 161-80.

31 Jungermann K, Kietzmann T. Zonation of parenchymal and nonparenchymal metabolism in liver. *Annu.Rev.Nutr.* 1996; 16: 179-203.

32 Wu TK, Wang YK, Chen YC, Feng JM, Liu YH, Wang TY. Identification of a Vibrio furnissii oligopeptide permease and characterization of its in vitro hemolytic activity. *J.Bacteriol.* 2007; 189: 8215-23.

33 Wang YK, Huang SC, Wu YF, Chen YC, Lin YL, Nayak M, Lin YR, Chen WH, Chiu YR, Li TT, Yeh BS, Wu TK. Site-directed mutations of thermostable direct hemolysin from Grimontia hollisae alter its arrhenius effect and biophysical properties. *Int.J.Biol.Sci.* 2011; 7: 333-46.

34 Tatsumi M, Nakamoto Y, Traughber B, Marshall LT, Geschwind JF, Wahl RL. Initial experience in small animal tumor imaging with a clinical positron emission tomography/computed tomography scanner using 2-[F-18]fluoro-2-deoxy-D-glucose. *Cancer Res.* 2003; 63: 6252-7.